Journal of Medicinal Chemistry

Article

pubs.acs.org/jmc

Novel Colchicine-Site Binders with a Cyclohexanedione Scaffold Identified through a Ligand-Based Virtual Screening Approach

María-Dolores Canela,[†] María-Jesús Pérez-Pérez,[†] Sam Noppen,[‡] Gonzalo Sáez-Calvo,[§] J. Fernando Díaz,[§] María-José Camarasa,[†] Sandra Liekens,*[,‡] and Eva-María Priego*[,†]

[†]Instituto de Química Médica (IQM-CSIC), Juan de la Cierva 3, E-28006 Madrid, Spain

[‡]Rega Institute for Medical Research, KU Leuven, B-3000 Leuven, Belgium

[§]Centro de Investigaciones Biológicas (CIB-CSIC), Ramiro de Maeztu 9, E-28040 Madrid, Spain

Supporting Information

ABSTRACT: Vascular disrupting agents (VDAs) constitute an innovative anticancer therapy that targets the tumor endothelium, leading to tumor necrosis. Our approach for the identification of new VDAs has relied on a ligand 3-D shape similarity virtual screening (VS) approach using the ROCS program as the VS tool and as query colchicine and TN-16, which both bind the α,β-tubulin dimer. One of the hits identified, using TN-16 as query, has been explored by the synthesis of its structural analogues, leading to 2-(1-((2-methoxyphenyl)amino)ethylidene)-5-phenylcyclohexane-1,3-dione (compound **16c**) with an $IC_{50} = 0.09 \pm 0.01$ μM in HMEC-1 and BAEC, being 100-fold more potent than the initial hit. Compound **16c** caused cell cycle arrest in the G2/M phase and interacted with the colchicine-binding site in tubulin, as confirmed by a competition assay with *N,N′*-ethylenebis(iodoacetamide) and by fluorescence spectroscopy. Moreover, **16c** destroyed an established endothelial tubular network at 1 μM and inhibited the migration and invasion of human breast carcinoma cells at 0.4 μM. In conclusion, our approach has led to a new chemotype of promising antiproliferative compounds with antimitotic and potential VDA properties.

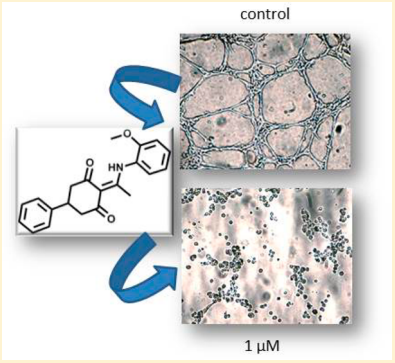

INTRODUCTION

The growth of solid tumors and development of metastasis are highly dependent on the existence of a vascular network that provides oxygen and nutrients.[1] Therefore, antivascular strategies are increasingly gaining importance among antineoplastic therapies and represent a new frontier in the treatment of cancer.[2] Basically, there are two major approaches in antivascular therapies: antiangiogenic drugs, which inhibit new blood vessel formation,[3] and vascular-disrupting agents or VDAs, which affect the existing vasculature.[4,5] While antiangiogenic drugs are mostly cytostatic to the endothelial cells and need to be chronically administered, VDAs are typically cytotoxic and cause a quick and dramatic collapse in the blood flow that leads to ischemia and necrosis just 24 h after administration. Thus, they are particularly effective in advanced stages when large tumors are formed. Importantly, one of the main advantages of such antivascular approaches is that they target endothelial cells, a cell population less prone to mutations than tumor cells.[6]

The selectivity of VDAs for tumor endothelium versus physiological vessels lies in the crucial differences between them.[7] In fact, tumor vessels are characterized by a higher proliferation rate, absence of pericytes, basal membrane deficiencies, and increased vascular permeability. Moreover, tumor vessels are more fragile and tortuous, which results in a higher resistance to blood flow. This makes them more sensitive to any decrease in perfusion pressure.[8]

Besides biotechnological approaches, involving immunotoxins and targeted antibodies, there is an increasing interest in low-molecular-weight molecules that behave as VDAs, and some of them are in clinical trials for a variety of solid tumors.[9] The best-studied VDAs are microtubule-destabilizing agents that bind the α,β-tubulin dimer at the colchicine-binding site.[10] The most representative compounds include colchicine (**1**); ZD6126 (**2**); ABT-751 (**3**); combrestastatins and their prodrugs, CA1P (**4a**), CA4P (**4b**), and AVE-8062 (**4c**); indibulin (**5**), and CI-980 (**6**), as shown in Figure 1. These compounds inhibit tubulin polymerization in endothelial cells, affecting the cellular cytoskeleton and therefore induce changes not only in the shape of endothelial cells but also in their motility, invasion, attachment, and proliferation.[11,12] As a result of a large cascade of events, such as actin stress fiber contraction and the subsequent activation of Rho kinases, VDAs lead to vascular collapse, tumor hypoxia, and hemorrhagic necrosis.[13]

It is interesting to mention that colchicine-like VDAs are able to behave as antimitotic agents at concentrations slightly higher than those at which the antivascular effects are observed. This

Received: October 21, 2013
Published: April 28, 2014

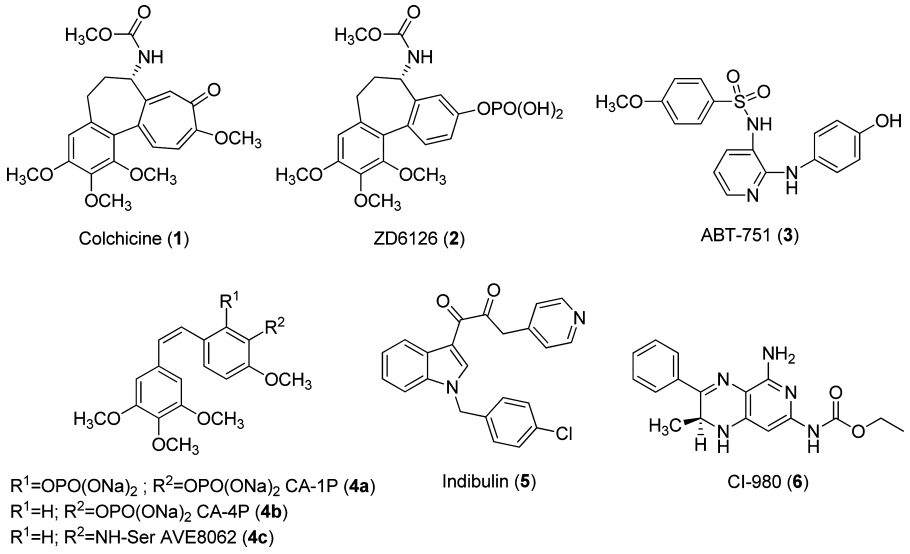

Figure 1. Chemical structures of selected colchicine-site binders.

antimitotic effect, closely related to the importance of the cytoskeleton of α,β-tubulin in mitotic spindle formation, when affecting tumor cells, may induce apoptosis. Therefore, this dual mechanism of action affecting endothelial and tumor cells makes these drugs very promising for anticancer therapy.[14]

Despite the great potential of these drugs, they suffer some drawbacks. In particular, colchicine is too toxic to be considered a suitable anticancer drug,[15] and CA-4P presents chemical instability, leading to the inactive trans-isomer, and shows a short biological half-life.[16]

Therefore, our objective has been to identify new chemical entities able to bind at the colchicine-binding site in α,β-tubulin that may lead to a novel type of compound with antiproliferative and antivascular properties. To address this aim, we relied on a ligand-based virtual screening (VS) approach.[17] Such an approach represents a quick, efficient, and well-documented strategy to access novel active molecules for a particular target. Among the computational methods available for this strategy, we have focused on 3-D shape similarity, a strategy successfully applied on recently reported examples.[18] A significant advantage of this approach is that no specification of the chemical structure (i.e., types of atoms and/or their bond arrangements) is required; thus, chemical scaffolds significantly different from the template can be identified.

Here we report the results obtained after conducting a ligand-based VS campaign using two different queries, identification of the hits, further exploration in terms of improvement of their antiproliferative properties, and determination of the mechanism of action.

RESULTS AND DISCUSSION

Virtual Screening. The virtual screening protocol employed is summarized in Figure 2, and all details are described in the Experimental Section.

The compounds for the virtual screening were obtained from the freely available ZINC database,[19] (version 8, which comprises about 8.5 million molecules) in SMILES format.[20] Prior to VS, the database was filtered on the basis of a customized "drug-like filter" using the software FILTER[21] to remove, among others, compounds with reactive functional

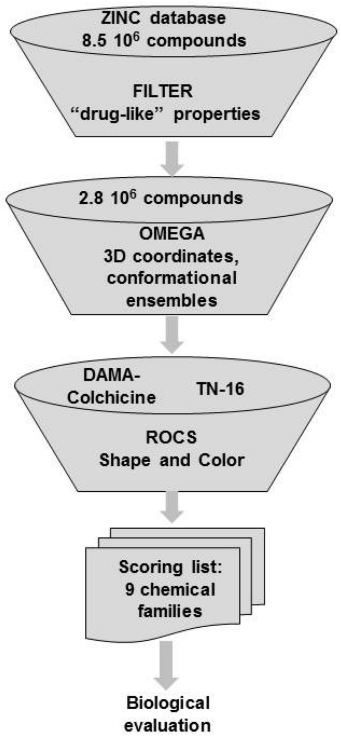

Figure 2. Schematic view of the virtual screening protocol.

groups. The filtered database was subjected to OMEGA[22] to generate the 3D atomic coordinates and conformational ensembles of all the compounds. As a tool for the VS, we have used ROCS,[23] a shape comparison program based on the concept that molecules have a similar shape if their volumes, represented by a Gaussian function, overlay well.[24,25] Besides shape comparison, an electrostatic complementary term called "color", which represents chemical similarity, was also applied.

As the query against which the comparison was performed, the 3-D structures of two well-known tubulin binders at the colchicine site were used: a colchicine derivative (DAMA-colchicine, **7**)[26] and TN-16 (**8**)[27] (Figure 3A). A superposition of their experimental cocrystal structures with α,β-tubulin is shown in Figure 3B, and a closer view of the overlap of the

dx.doi.org/10.1021/jm401939g | J. Med. Chem. 2014, 57, 3924−3938

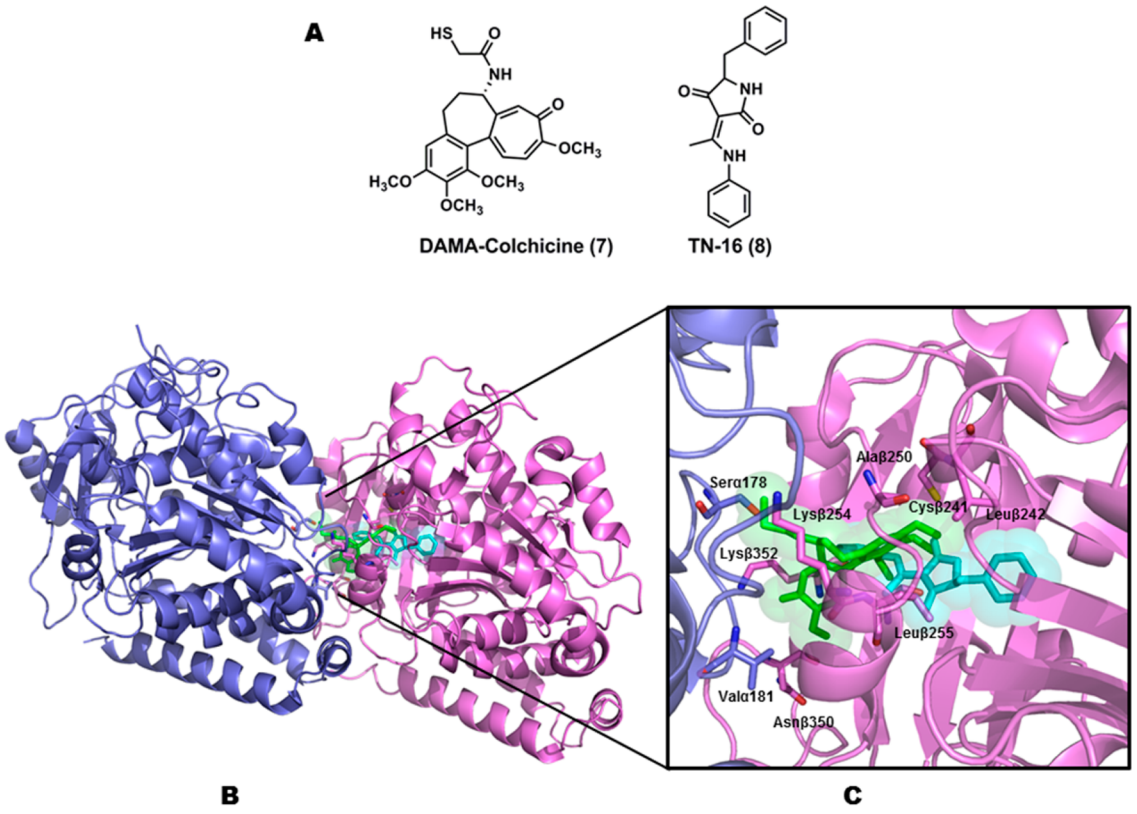

Figure 3. (A) Chemical structures of DAMA-colchicine (**7**) and TN-16 (**8**). (B) Colchicine binding-site in the α,β-tubulin dimer. (C) Superposition of the ligands used in the VS: DAMA-colchicine (green, PDB ID 1sa0) and TN-16 (cyan, PDB ID 3hkd). Key residues in the binding site are shown and labeled.

ligands is found in Figure 3C. The X-ray of the complex tubulin−TN-16, reported in 2009, clearly shows that this compound is more deeply buried in the β-monomer than DAMA-colchicine. Therefore, TN-16 explores a pocket partially different from that of colchicine in the so-called colchicine-binding domain.[27]

The VS protocol included shape comparison and scoring, "color" comparison and scoring (shape plus color), and finally visual inspection. On the basis of previously reported examples,[25] we established a Tanimoto score of 0.75 for the shape comparison, and a "Combo-score" of 1.4 for the sum of shape and color comparison.

When using DAMA-colchicine as query and the cutoff values mentioned above, the highest hits in the scoring list showed structures that closely resembled colchicine or other described tubulin inhibitors; thus, no novel scaffolds were identified using our protocol. Alternatively, when TN-16 was used as template, the scoring list revealed nine chemical families of compounds that had not been previously described in the literature as tubulin binders. On the basis of compound availability, a total of six representative examples of these families (see Table S1 in the Supporting Information) were purchased and evaluated for their antiproliferative activity against one endothelial cell line (MBEC) and one tumor cell line (L1210). From the compounds tested (Table S2 in the Supporting Information) only the cyclohexanedione **9** (Figure 4) showed significant inhibition of cell proliferation in both cell lines with IC_{50} values of 13 ± 5 μM. Evaluation of **9** against four other cell lines indicated similar IC_{50} values. In addition, binding of the hit compound **9** to tubulin at the colchicine site was confirmed by the displacement of 2-methoxy-5-(2,3,4-trimethoxyphenyl)-2,4,6-cycloheptatrien-1-one (MTC, a reversible colchicine-binding site ligand) as determined by fluorescence spectroscopy (see Figure S1 in the Supporting Information). Moreover, and from a chemical point of view, compound **9** was considered a suitable hit on the basis of its low molecular weight (335) and synthetic accessibility as described in the next section. Therefore, a synthetic-driven medicinal chemistry program was set up to evaluate structural analogues of **9**.

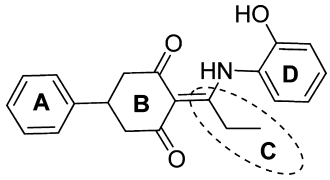

Figure 4. Structure of the hit compound **9** identified from the VS campaign.

Chemistry. Since the hit compound **9** had been acquired from a commercial source, the first task was to devise a synthetic strategy that could allow the exploration of the different fragments of the molecule (Figure 4), in particular, the aromatic rings **A** and **D** and the alkyl chain **C**, while the cyclohexanedione **B** was kept as a common structural motif. This strategy consisted of the reaction of the 5-substituted cyclohexane-1,3-diones (representing fragments **A** and **B**) with acyl chlorides to obtain the *C*-acyl derivatives followed by Schiff base formation with anilines (fragment **D**). Since fragment **D** was the last structural element incorporated in this synthetic strategy, the first series of modifications were performed on this fragment.

dx.doi.org/10.1021/jm401939g | J. Med. Chem. 2014, 57, 3924−3938

Scheme 1[a]

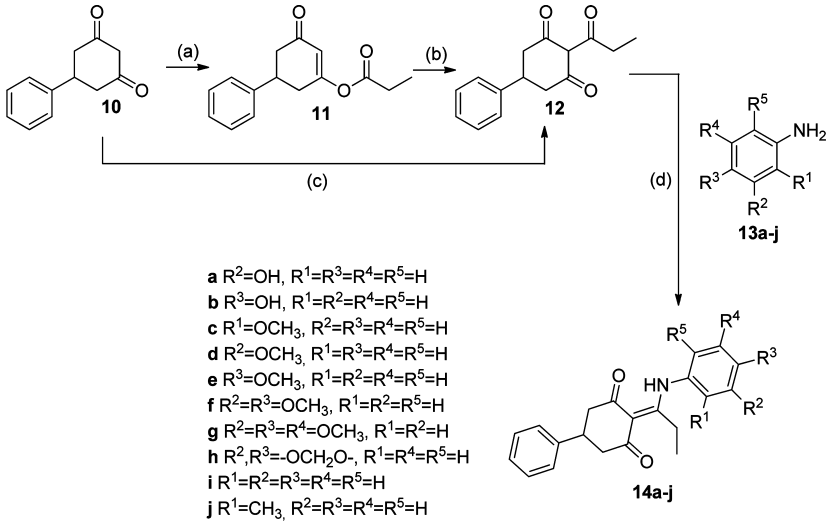

[a]Reagents and conditions: (a) DMAP, DIPEA, CH_2Cl_2, 70 °C, 2 h, 64% yield; (b) anhyd K_2CO_3, 1,2,4-triazole, CH_3CN, 30 °C, >48 h, 30% yield; (c) anhyd K_2CO_3, 1,2,4-triazole, Bu_4NBr, CH_3CN, microwave irradiation (MW), 70 °C, 2 h, 51% yield; (d) toluene, 4 Å molecular sieves, MW, 150 °C, 2 h, 30–98% yields.

Thus, reaction of the commercially available 5-phenylcyclohexane-1,3-dione (**10**) with propionyl chloride in dichloromethane in the presence of DMAP and DIPEA at 70 °C (Scheme 1) as described for similar analogues[28] afforded the *O*-acyl derivative **11** in 64% yield but not the *C*-acyl derivative **12** as expected. Interestingly, similar *O*-acyl derivatives have been transformed into the corresponding *C*-isomers by reaction with K_2CO_3 in acetonitrile in the presence of 1,2,4-triazole, by varying the temperature between −10 and 100 °C or by phase-transfer catalysis.[29] When compound **11** was treated with K_2CO_3 in acetonitrile in the presence of 1,2,4-triazole at 30 °C, only 30% of the *C*-analogue **12** was obtained after 48 h of reaction. However, with this information, we assayed new reaction conditions meant to perform these two steps in a "one-pot" procedure and made use of microwave-assisted irradiation to reduce the reaction times. Thus, reaction of **10** with propionyl chloride in CH_3CN under microwave conditions in the presence of K_2CO_3, 1,2,4-triazole, and Bu_4NBr as a phase transfer catalyst at 70 °C afforded the corresponding *C*-propionyl derivative **12** in 51% yield. It should be mentioned that the combination of phase transfer catalysis and microwave irradiation afforded the desired *C*-acyl derivative in just a couple of hours, and to the best of our knowledge, this methodology has never been applied to this type of reaction.

Then reaction of **12** with anilines carrying OH or OMe groups in toluene at 150 °C for 2 h under microwave radiation in the presence of 4 Å molecular sieves yielded compounds **14a–j.** The structures of **14a–j** were determined by ^1H and ^{13}C NMR, HMBC, and HSQC correlation experiments. It should be emphasized that, in the ^1H NMR spectra, a broad singlet appeared around 15 ppm, corresponding to the NH group. This chemical shift suggested the participation of the NH in a potential hydrogen bond with one of the carbonyl groups of the 1,3-cyclohexanedione. To further explore this issue, the ^1H NMR spectra of compound **14c** was recorded in DMSO-d_6 and $CDCl_3$, and in both cases, the NH signal remained almost unaffected (δ 14.7 ppm). Additionally, a 10-fold dilution of the sample with DMSO-d_6 did not affect the chemical shift of this signal, strongly suggesting the existence of an intramolecular hydrogen bond.

When tested for antiproliferative activity (see Table 1 and Biological Evaluation), compounds **14c** and **14j** afforded 2–30-fold lower IC_{50} values than the initial hit **9**. Therefore, we decided to explore the length of the alkyl chain in fragment **C** while an OMe or Me was kept in the *ortho* position of the **D** aromatic ring (Scheme 2). Thus, reaction of the cyclohexanedione **10** with butyryl or acetyl chloride in the presence of K_2CO_3, 1,2,4-triazole, Bu_4NBr in acetonitrile under microwave conditions afforded the *C*-acyl derivatives **15a** and **15b**, respectively. Further reaction of these acyl derivatives with *o*-toluidine or *o*-anisidine in toluene afforded compounds **16a–d** in excellent yields.

When compounds **16a–d** were tested for antiproliferative activity (see Table 1 and Biological Evaluation), derivatives **16c** and **16d** with a methyl at fragment **C** afforded the best inhibitory values. With this information and keeping a methyl as side chain in **C**, a wider battery of anilines was introduced at fragment **D** with at least one substituent at position 2 of the aromatic ring. Therefore, as shown in Scheme 3, reaction of 2-acetyl-5-phenylcyclohexane-1,3-dione (**15b**) with commercially available 2-chloro (**17a**), 2-fluoro (**17b**), 2-trifluoromethyl (**17c**), 2,3-difluoro (**17d**), 2,6-difluoro (**17e**), 2,5-dimethoxy (**17f**), and 2,6-dimethoxy (**17g**) anilines afforded compounds **18a–g**.

The next series of modifications affected fragment **A** by replacing the phenyl ring by other groups, in particular, a cyclohexyl, a benzyl, or a *gem*-dimethyl (Scheme 4). The cyclohexane-1,3-diones with a cyclohexyl or a benzyl at position 5 (**21a** and **21b**) were synthesized through the α,β-unsaturated ketone precursors (**20a** and **20b**) that were obtained following two different approaches. The synthesis of **20a** was undertaken by condensation between cyclohexane carbaldehyde (**19a**) and acetone under basic conditions,[30] while the benzyl derivative **20b** was obtained by a Witting reaction of phenylacetaldehyde (**19b**) with 1-(triphenylphosphoranylidene)-2-propenone in chloroform following described procedures.[31] Then **20a** and **20b** were allowed to react with diethylmalonate in the presence

dx.doi.org/10.1021/jm401939g | J. Med. Chem. 2014, 57, 3924–3938

Table 1. Antiproliferative Activity of Cyclohexanedione Derivatives in Endothelial and Tumor Cell Lines

	endothelial cells IC_{50} (μM)			tumor cells IC_{50} (μM)		
compd	HMEC-1	MBEC	BAEC	L1210	CEM	HeLa
colchicine	0.0038 ± 0.0011	0.031 ± 0.015	0.0069 ± 0.0008	0.010 ± 0.001	0.013 ± 0.001	0.0087 ± 0.0001
9	22 ± 13	13 ± 5	35 ± 1	13 ± 1	15 ± 9	11 ± 8
14a	13 ± 6	12 ± 3	7.8 ± 0.9	15 ± 12	48 ± 26	75 ± 25
14b	28 ± 21	18 ± 0	36 ± 2	14 ± 7	34 ± 0	79 ± 42
14c	1.4 ± 0.2	1.4 ± 0.1	1.2 ± 0.6	1.5 ± 0.2	2.3 ± 1.7	4.3 ± 0.7
14d	18 ± 9	16 ± 4	64 ± 14	32 ± 9	45 ± 12	66 ± 9
14e	≥100	57 ± 7	≥100	58 ± 13	67 ± 11	≥100
14f	>100	>100	>100	>100	>100	>100
14g	>100	>100	>100	>100	>100	>100
14h	53 ± 11	50 ± 18	43 ± 6	38 ± 0	53 ± 22	76 ± 5
14i	15 ± 6	8.3 ± 2.1	16 ± 11	22 ± 17	21 ± 11	56 ± 3
14j	2.1 ± 2.0	2.8 ± 0.2	2.2 ± 0.2	6.9 ± 1.5	6.3 ± 1.2	9.2 ± 5.0
16a	31 ± 3	27 ± 4	16 ± 3	36 ± 8	41 ± 1	59 ± 23
16b	44 ± 2	47 ± 3	46 ± 4	41 ± 19	≥100	>100
16c	0.09 ± 0.01	0.12 ± 0.01	0.09 ± 0.01	0.16 ± 0.08	0.18 ± 0.05	0.18 ± 0.00
16d	0.26 ± 0.08	0.32 ± 0.04	0.17 ± 0.03	0.30 ± 0.18	0.68 ± 0.09	0.48 ± 0.26
18a	0.56 ± 0.16	0.47 ± 0.05	0.29 ± 0.03	0.70 ± 0.62	0.64 ± 0.18	0.71 ± 0.20
18b	0.93 ± 0.46	1.0 ± 0.1	0.51 ± 0.01	1.9 ± 0.7	1.1 ± 0.3	3.4 ± 2.4
18c	7.7 ± 2.1	8.7 ± 0.1	8.1 ± 0.5	14 ± 10	18 ± 2	32 ± 18
18d	10 ± 2	12 ± 0	14 ± 2	19 ± 1	25 ± 18	36 ± 3
18e	6.6 ± 0.5	9.2 ± 1.8	8.4 ± 1.5	11 ± 2	21 ± 6	17 ± 4
18f	2.6 ± 0.2	3.2 ± 0.2	2.6 ± 0.5	36 ± 22	6 to >100[a]	46 ± 3
18g	1.4 ± 0.8	1.2 ± 0.2	0.46 ± 0.29	1.0 ± 0.0	1.4 ± 0.7	1.1 ± 0.2
23a	12 ± 1	21 ± 5	12 ± 1	8 to >100[a]	15 ± 6	11 ± 5
23b	22 ± 2	87 ± 15	>100	>100	>100	>100
23c	76 ± 18	71 ± 41	48 ± 11	>100	>100	>100
26a	5.8 ± 0.4	6.8 ± 0.8	3.2 ± 0.2	11 ± 0	7.2 ± 0.2	13 ± 3
26b	4.3 ± 0.3	5.4 ± 0.6	2.7 ± 0.2	6.3 ± 0.6	4.9 ± 1.4	4.8 ± 0.1
26c	35 ± 1	39 ± 2	41 ± 2	24 ± 3	23 ± 0	55 ± 27
26d	39 ± 8	60 ± 9	>100	>100	>100	>100
26e	0.33 ± 0.12	0.42 ± 0.01	0.26 ± 0.07	0.17 ± 0.11	0.31 ± 0.07	0.79 ± 0.12
26f	0.30 ± 0.08	0.41 ± 0.08	0.23 ± 0.09	0.21 ± 0.09	0.24 ± 0.10	0.69 ± 0.01
26g	11 ± 3	9.2 ± 1.1	8.4 ± 0.2	>100	>100	90 ± 4
26h	>100	>100	>100	>100	>100	>100
26i	55 ± 16	46 ± 1	42 ± 1	22 ± 0	28 ± 8	58 ± 23
26j	1.8 ± 0.1	2.1 ± 0.1	1.7 ± 0.4	3.3 ± 0.4	5.3 ± 1.0	4.0 ± 0.4
26k	0.67 ± 0.07	0.64 ± 0.05	0.48 ± 0.04	0.26 ± 0.22	0.72 ± 0.25	0.66 ± 0.03
26l	2.2 ± 0.6	2.5 ± 0.2	2.1 ± 0.1	3.5 ± 1.7	6.2 ± 0.2	4.1 ± 0.2

[a]Indicates no dose–response in the indicated concentration range, making accurate IC_{50} calculation impossible.

Scheme 2[a]

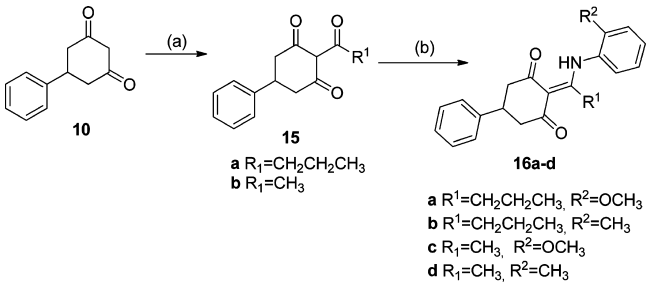

[a]Reagents and conditions: (a) R^1COCl, anhyd K_2CO_3, 1,2,4-triazole, Bu_4NBr, CH_3CN, MW, 70 °C, 2 h (**15a**, 29% yield; **15b**, 54% yield); (b) substituted aniline, toluene, molecular sieves, MW, 150 °C, 2 h, 60–84% yields.

Scheme 3[a]

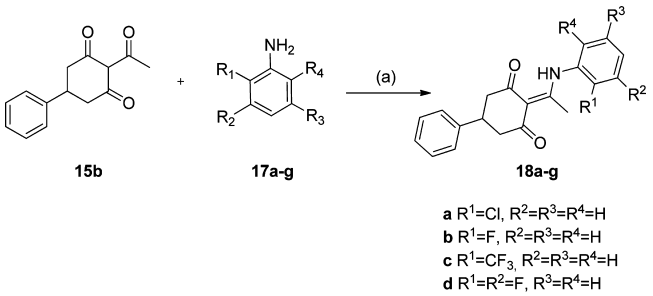

[a]Reagents and conditions: (a) toluene, molecular sieves, MW, 150 °C, 2 h, 23–78% yields.

of sodium ethoxide in ethanol at 60 °C[30] to afford the cyclohexane-1,3-diones **21a** and **21b**, respectively. *C*-Acylation

dx.doi.org/10.1021/jm401939g | J. Med. Chem. 2014, 57, 3924–3938

Scheme 4[a]

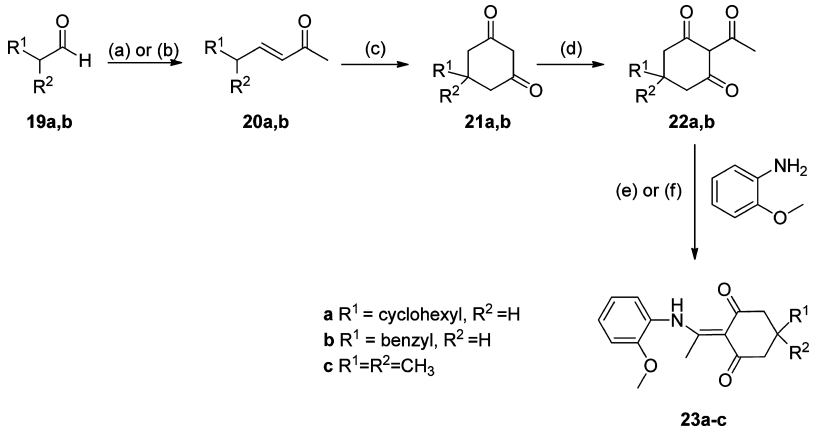

[a]Reagents and conditions: (a) NaOH (1%), acetone, H_2O, rt, overnight (for **20a**, 65% yield); (b) $Ph_3P{=}CHCOCH_3$, $CHCl_3$, 60 °C, 4 h (for **20b**, 77% yield); (c) (i) diethyl malonate, EtONa, EtOH, Δ; (ii) NaOH, 80 °C, 2 h; (iii) HCl, Δ, 1 h (for **21a**, 69% yield; for **21b**, 33% yield); (d) $ClCOCH_3$, anhyd K_2CO_3, 1,2.4-triazole, Bu_4NBr, CH_3CN, MW, 70 °C, 2 h (for **22a**, 36% yield; for **22b**, 38% yield; **22c** was commercially available); (e) toluene, molecular sieves, pressure tube, 110 °C, overnight (for **23a**, 89% yield; for **23b**, 73% yield); (f) toluene, molecular sieves, MW, 150 °C, 2 h (for **23c**, 79% yield).

Scheme 5[a]

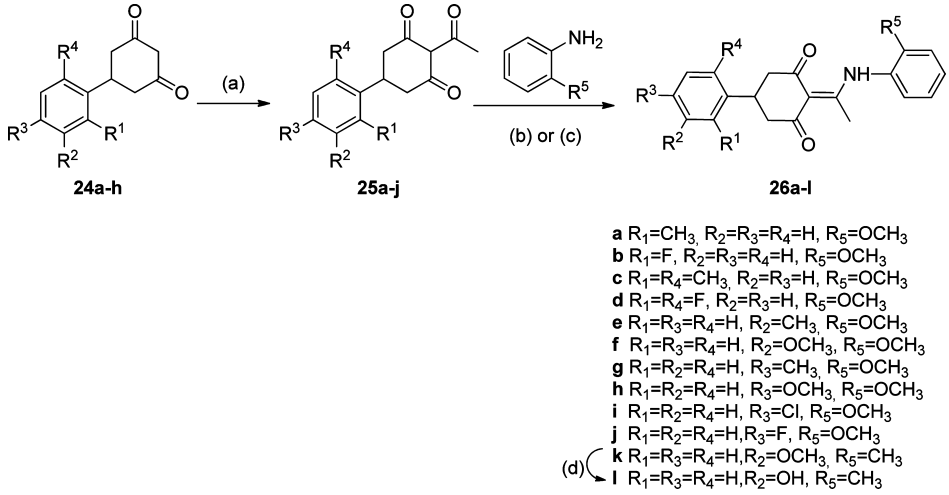

[a]Reagents and conditions: (a) CH_3COCl, anhyd K_2CO_3, 1,2,4-triazole, Bu_4NBr, CH_3CN, MW, 70 °C, 2 h, 14−74% yields; (b) for **26e−j**, toluene, molecular sieves, MW 150 °C, 2 h, 39−99% yields; (c) for **26a-d,k**, toluene, molecular sieves, pressure tube, 110 °C, overnight, 39−75% yields; (d) BBr_3, CH_2Cl_2, rt, 12 h, 23% yield.

of **21a** and **21b** with acetyl chloride, as described in previous examples, and further reaction with *o*-anisidine afforded **23a** and **23b** in excellent yields. Similarly, reaction of the commercially available *gem*-dimethyl derivative **22c** with *o*-anisidine in toluene at reflux afforded **23c**. It should be mentioned that these compounds were poorly active, pointing to the importance of the aromatic ring directly attached to the cyclohexanedione for the antiproliferative activity

Thus, with a phenyl group kept at **A**, a variety of substituents was introduced on this ring. The 5-phenylcyclohexane-1,3-diones **24a−h** (Scheme 5) were synthesized from the corresponding substituted benzaldehydes following described procedures,[32,33] in a similar way to that described in Scheme 4. *C*-Acylation of **24a−h** with acetyl chloride and further reaction with *o*-anisidine or *o*-toluidine provided compounds **26a−k**. Finally, demethoxylation of **26k** with BBr_3 in CH_2Cl_2 at room temperature afforded the corresponding hydroxyl derivative **26l**.

Biological Evaluation. *Antiproliferative Activity.* The synthesized compounds were evaluated for their antiproliferative activity in six different cell lines: three endothelial cell lines [human microvascular endothelial cells (HMEC-1), mouse brain endothelial cells (MBEC), and bovine aortic endothelial cells (BAEC)] and three cancer cell lines [mouse lymphocytic leukemia (L1210), human lymphoblastic leukemia (CEM), and human cervical carcinoma (HeLa) cells].[34] Data are expressed as IC_{50} (50% inhibitory concentration) defined as the concentration at which the compounds reduce cell proliferation by 50% and are shown in Table 1. As reference compound we included colchicine (**1**), which inhibited proliferation of the different cell lines with IC_{50} values ranging from 0.0038 to 0.031 μM.

Those compounds with an OH at position *ortho*, *meta*, or *para* in fragment **D** (**9**, **14a**, or **14b**) were moderately active in the different cell lines, with IC_{50} values ranging from 8 to 36 μM in endothelial cells and from 11 to 79 μM in the tumor cell

dx.doi.org/10.1021/jm401939g | J. Med. Chem. 2014, 57, 3924−3938

lines. However, compounds with an OMe at these positions showed a more diverse behavior in terms of antiproliferative activity. Thus, the *p*-OMe compound (**14e**) was marginally active in some cell lines ($IC_{50} \geq 57$ μM) and the *m*-OMe derivative (**14d**) showed moderate activity (IC_{50} of 16−66 μM), while the *o*-OMe isomer (**14c**) afforded IC_{50} values of 1.2−4.3 μM, that is, 10−30-fold better than the hit compound **9** in endothelial cells. The double or triple substituted compounds (**14f**, **14g**, or **14h**) were inactive or poorly active. The unsubstituted compound (**14i**) showed moderate antiproliferative activity, while the *o*-CH_3 derivative (**14j**) was as active as the corresponding *o*-OMe compound **14c**.

The length of the alkyl chain in fragment **C** was varied while an OMe or Me was kept in the *ortho* position of the **D** aromatic ring. The resulting propyl derivatives **16a** and **16b** showed moderate antiproliferative activity, with IC_{50} values at least 13-fold higher than those of the corresponding ethyl derivatives **14c** and **14j**. Interestingly, the methyl derivatives **16c** and **16d** were significantly more active than the corresponding ethyl derivatives, with IC_{50} values as low as 0.09 and 0.18 μM for compound **16c** in endothelial and tumor cells, respectively. Depending on the cell line, this represents a 60- (HeLa cells) to 400-fold (BAEC) increase in the antiproliferative effect compared with the initial hit. Thus, methyl was selected as the substituent of choice in fragment **C**.

Keeping a methyl group as the alkyl chain at fragment **C**, we further explored the *ortho* position in fragment **D** by incorporating different electron-withdrawing groups. Thus, introduction of a chlorine (**18a**) afforded IC_{50} values in the sub-micromolar range (0.3−0.7 μM), whereas a fluorine (**18b**) resulted in slightly increased IC_{50} values (0.5−3.4 μM) and the *o*-trifluoromethyl derivative **18c** lost 10-fold activity (IC_{50} of 8−32 μM). Interestingly, the disubstituted derivatives [2,3-difluoro (**18d**), 2,6-difluoro (**18e**), and 2,5-dimethoxy (**18f**)] were all moderate inhibitors of cell growth, being less potent than the related *ortho*-monosubstituted compounds (i.e., **18b** and **16c**, respectively), whereas the 2,6-dimethoxy derivative (**18g**) showed comparable activity as **18b**.

Concerning fragment **A**, substitution of the phenyl ring by a cyclohexyl (compare **16c** and **23a**) resulted in at least 10-fold higher IC_{50} values. Replacement by a benzyl or a *gem*-dimethyl (compounds **23b** and **23c**) was even more detrimental for activity, suggesting the importance of an aromatic ring directly attached to the cyclohexane-1,3-dione. Finally, we introduced a variety of substituents at this phenyl ring (compounds **26a−l**, Table 1). Compounds substituted with Me or F at the *ortho* position in fragment **A** (**26a** and **26b**) showed some antiproliferative activity against the different cell lines, but at IC_{50} values 50-fold higher than the unsubstituted phenyl derivative **16c**. Introduction of a double substitution at positions 2 and 6 either with methyl or fluorine (**26c** and **26d**, respectively) reduced the antiproliferative effect even more. On the other hand, the *meta*-substituted compounds **26e**, **26f**, and **26k** were nicely active in all cell lines with IC_{50} values around 0.17−0.79 μM. Only compound **26l**, with an OH at the *meta* position, was less active, with an IC_{50} value in the low micromolar range. Finally, the *para*-substituted compounds showed only very moderate antiproliferative activity, the only exception being **26j**, containing a fluorine, that was still 20-fold less active than the unsubstituted compound **16c**.

From this evaluation some structural requirements for antiproliferative activity among this family of compounds can be extracted: (i) the aromatic ring **D** needs to be substituted at the *ortho* position with either a methoxy, a methyl, a chloro, or, to a lesser extent, a fluoro; (ii) the optimal alkyl chain at fragment **C** seems to be one carbon atom; (iii) fragment **A** must be a phenyl, preferentially unsubstituted or with a methyl or methoxy at the *meta* position.

A number of in vitro experiments were then carried out to elucidate the mechanism of action of these new antiproliferative compounds. Colchicine was included as positive control.

Inhibition of Cell Cycle Progression. To investigate at which phase of the cell cycle the compounds exert their antimitotic effect, we performed cell cycle analysis on HMEC-1 treated with six of the most potent compounds (**16c**, **16d**, **18a**, **18b**, **26e**, and **26f**).[35] Thus, HMEC-1 cells were incubated in the presence of different concentrations of colchicine or tested compound for 24 h, after which cell cycle distribution was measured by flow cytometry. The results obtained for compounds **16c**, **16d**, and colchicine (**1**) are shown in Figure 5. Untreated cells showed a classical pattern of proliferating

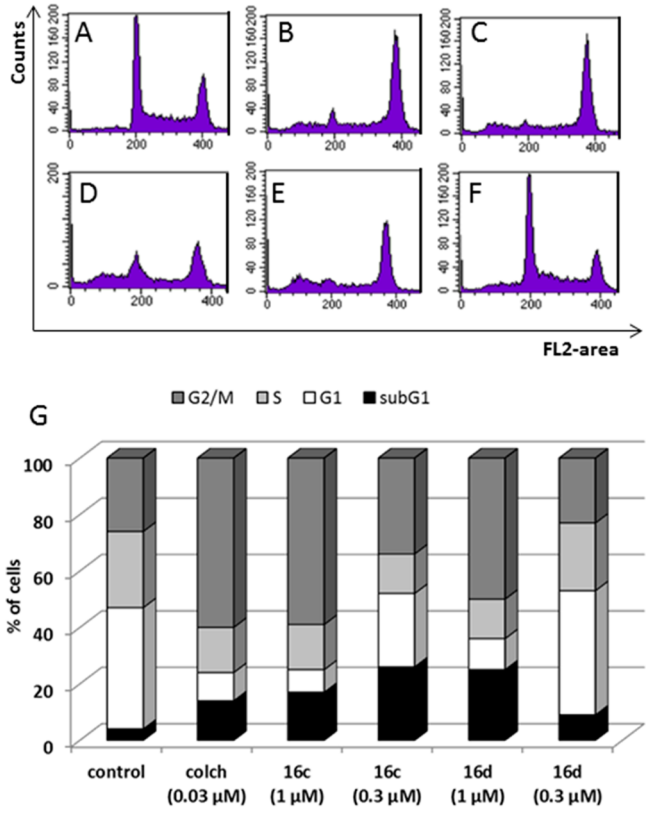

Figure 5. Cell cycle distribution. HMEC-1 cells were treated with DMSO (A), colchicine [0.03 μM (B)], **16c** [1 μM (C) or 0.3 μM (D)], or **16d** [1 μM (E) or 0.3 μM (F)] for 24 h. Next, the cells were harvested and stained with propidium iodide, and cell cycle distribution was evaluated by flow cytometry. Percentages of cells in the different phases of the cell cycle are indicated (G).

cells distributed in the G1, S, and G2/M phase. When these cells were treated with 0.03 μM colchicine, an accumulation in G2/M phase and an increase in subG1 cells undergoing apoptosis were observed. A similar effect was noted in the presence of the test compounds, although at higher concentrations; compound **16c** caused G2/M phase arrest and apoptosis at 0.3 μM, while at least 1 μM of the other inhibitors was needed to exert a comparable activity. Therefore, **16c** was the compound of choice for subsequent experiments.

dx.doi.org/10.1021/jm401939g | J. Med. Chem. 2014, 57, 3924−3938

Tubulin Binding. VDAs, including colchicine, arrest cell cycle progression at G2/M phase by interfering with tubulin polymerization. In order to evaluate whether our compounds bind to tubulin we carried out a recently described competition assay with *N,N′*-ethylene-bis(iodoacetamide) (EBI) in human breast cancer MDA-MB-231 cells.[36] EBI is an alkylating agent that specifically binds to two cysteine residues present in the colchicine-binding site of tubulin, Cys239 and Cys354. This β-tubulin adduct can be detected by Western blot as a second immunoreactive β-tubulin band that migrates faster than β-tubulin itself. So, if EBI is added to cells previously treated with a colchicine-site binder, the binding site is already occupied and the EBI adduct cannot be observed. Since the distance between the different bands depends on the cell type, we used MDA-MB-231 cells in which the two bands can be easily distinguished. As shown in Figure 6, addition of EBI led to

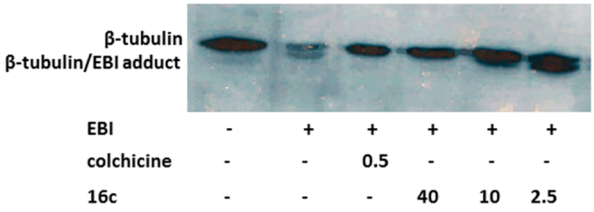

Figure 6. Inhibition of tubulin binding by **16c**. MDA-MB-231 cells were treated with DMSO, colchicine (0.5 μM), or **16c** (40, 10, or 2.5 μM) for 16 h. Next, EBI (100 μM) was added, and after 1.5 h, the cells were harvested and cell extracts were prepared for Western blot analysis using anti-β-tubulin antibody. EBI cross-links cysteine residues in β-tubulin, resulting in the formation of a β-tubulin adduct (second immunoreactive band) that migrates faster than β-tubulin. Compounds that bind to the colchicine-binding site in β-tubulin prevent the formation of the EBI:β-tubulin adduct.

the appearance of a second band below the β-tubulin band. Addition of colchicine (**1**) (0.5 μM) or **16c** (10 μM) prevented the covalent binding of EBI in living MDA-MB-231 cells, resulting in the absence of the adduct band. This effect was also observed in the presence of the other compounds (data not shown). Thus, these data indicate that our compounds induce their antimitotic effects by binding to the colchicine-binding site in β-tubulin.

Binding of some representative inhibitors (**14c**, **16c**, and **26f**) to tubulin was confirmed by competition with 2-methoxy-5-(2,3,4-trimethoxyphenyl)-2,4,6-cycloheptatrien-1-one (MTC) and (*R*)-(+)-ethyl 5-amino-2-methyl-1,2-dihydro-3-phenylpyrido[3,4-*b*]pyrazin-7-ylcarbamate (R-PT), two well-characterized, reversible colchicine-binding site ligands.[37−40] Indeed, all three compounds displace both MTC and R-PT, as determined by fluorescence spectroscopy (as shown in Figure S3 for **16c** in the Supporting Information).

In order to determine their binding affinities, competition experiments with MTC, the lower affinity compound (K_a = 4.7 × 10^5 M^{-1}),[41] were performed. The data indicated a very high affinity, making it difficult to precisely quantify the binding constant.[42] Therefore, the displacement of R-PT was used to measure the binding constants. First, we determined the binding constant of R-PT at 25 °C (5.1 × 10^6 M^{-1}), which was found to be 10 times higher than that of MTC and similar to the previously reported value (3.2 × 10^6 M^{-1}).[43] Then, R-PT displacement experiments were carried out with our three compounds allowing the determination of their binding affinities (Figure 7) in the sub-micromolar range (Table 2).

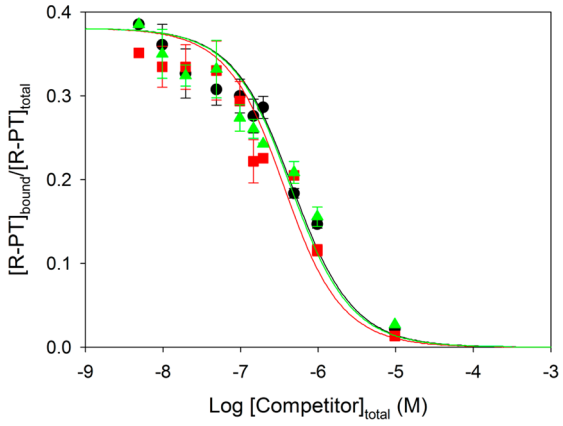

Figure 7. Displacement of the fluorescent probe R-PT (0.2 μM) bound to tubulin (0.2 μM) by **14c** (black lines and circles), **16c** (red lines and squares), and **26f** (green lines and triangles) at 25 °C. The solid lines were generated with the best fit value of the binding equilibrium constant of the competitors, assuming a one-to-one binding to the same site.

Table 2. Association Constants for Compounds 14c, 16c, and 26f and Other Colchicine-Binding Site Ligands

compd	K_{assoc} (M^{-1}) at 25 °C
colchicine	1.16 × 10^7 (at 37 °C)[a]
MTC	4.7 × 10^5 [b]
R-PT	3.2 × 10^6 [c]
podophyllotoxin	1.8 × 10^6 [d]
nocodazole	4 × 10^5 [e]
14c	(7.1 ± 1.2) × 10^6
16c	(9.6 ± 1.2) × 10^6
26f	(7.5 ± 0.76) × 10^6

[a]Data from ref 46. [b]Data from ref 40 [c]Data from ref 43. [d]Data from ref 45. [e]Data from ref 44.

Interestingly, the binding constants obtained are higher than those previously determined for other classical colchicine-binding site ligands, such as nocodazole (4 × 10^5 M^{-1})[44] or podophyllotoxin (1.8 × 10^6 M^{-1}).[45]

Inhibition of Mitotic Spindle Formation. Next, we investigated whether the interaction of the compounds with tubulin affects the organization of tubulin into mitotic spindles during cell division.[47] Therefore, MDA-MB-231 cells were treated with colchicine (0.1 μM) or **16c** (1 μM) for 8 h after which the microtubules were visualized by immunofluorescence microscopy (Figure 8). Whereas in the control cells (treated with 0.1% DMSO) chromosomes lined up along the metaphase plate and normal bipolar mitotic spindles extended from the cell poles toward the midpoint, highly aberrant, multipolar spindles were formed in the presence of colchicine or **16c**. Thus, the inability of the cells to proceed through the cell cycle after treatment with **16c** may be explained by the lack of DNA organization into a metaphase plate, which is required for proper cell division.

Antivascular Activity. Next, we studied the capacity of this new family of antiproliferative compounds to destroy a preexisting vasculature network formed by endothelial cells. HMEC-1 were seeded on top of matrigel, which induces their reorganization into tubelike structures within 3 h.[34] Then, colchicine (0.1−10 μM) or **16c** (0.1−10 μM) were added. After 90 min of treatment, the plates were photographed and the extent of tube formation was evaluated. As shown in Figure

dx.doi.org/10.1021/jm401939g | J. Med. Chem. 2014, 57, 3924−3938

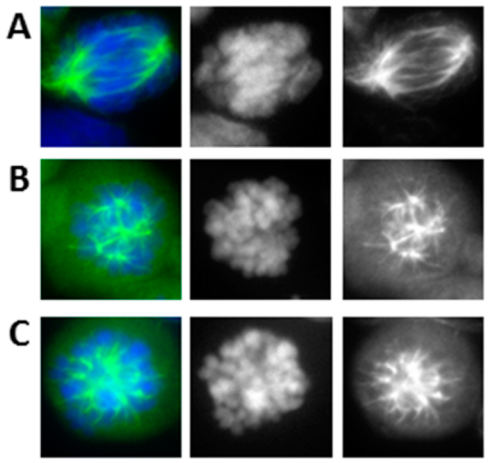

Figure 8. Inhibition of mitotic spindle formation. MDA-MB-231 cells were treated for 8 h with DMSO (A), colchicine (0.1 μM) (B), or **16c** (1 μM) (C), fixed, and stained with anti-β-tubulin antibody (green) to visualize the microtubules and with DAPI for DNA (blue). Column 1, double staining; column 2, DNA staining only; column 3, β-tubulin staining only.

9, colchicine significantly displayed vascular disrupting effects at 0.3 μM with total destruction of the cordlike structures at 1 μM. Similar effects were observed in the presence of **16c**, but at 3-fold higher concentration.

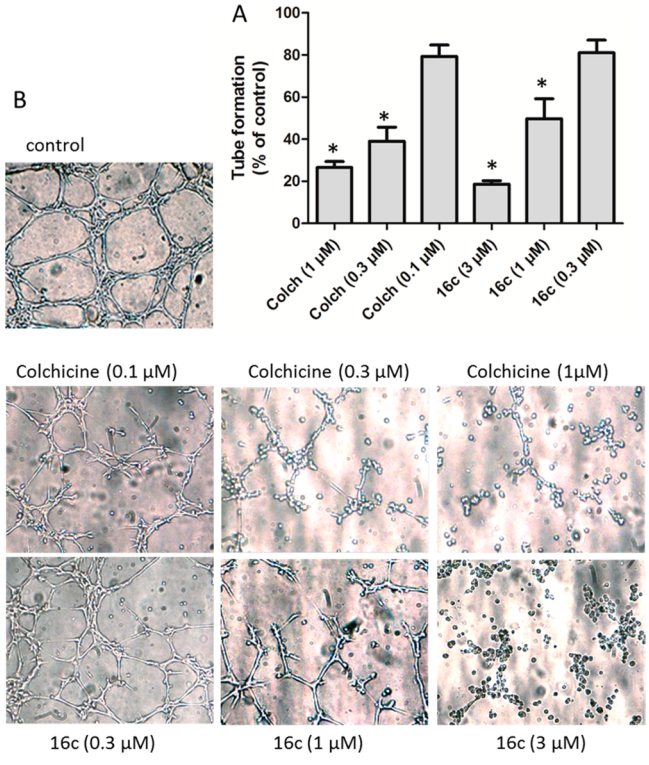

Figure 9. Vascular disrupting effects of **16c**. (A, B) HMEC-1 cells were cultured on matrigel for 3 h to allow the formation of tubelike structures. Then DMSO (0.1%) (control), colchicine (0.1, 0.3, or 1 μM), or **16c** (0.3, 1, or 3 μM) was added. After 90 min, tube formation was quantified. Values are expressed as mean ± SD of two independent experiments. *p < 0.05 compared with control with Student's t-test. Images show the vascular network after 90 min of treatment (B).

Migration and Invasion of MDA-MB-231 Cells. Tubulin-binding agents have been shown to inhibit the migratory and invasive properties of tumor cells.[48] Therefore, we investigated the ability of MDA-MB-231 breast carcinoma cells to migrate (or invade) through 8 μm (matrigel-coated) inserts in the presence of the compounds. As shown in Figure 10, colchicine

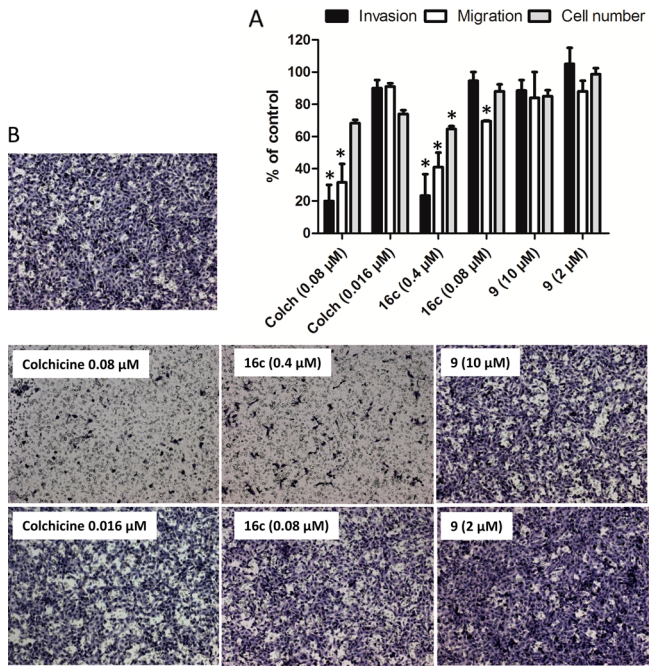

Figure 10. Inhibition of MDA-MB-231 cell migration and invasion by **16c**. MDA-MB-231 cells were seeded at 50 000 cells/insert in the presence of colchicine, **16c**, or **9**. After 17 h incubation, migrated cells were stained and counted. In parallel, cells were seeded at 50 000 cells/well (96-well plate) in the presence of the compounds. After 17 h, cells were counted. Data show biological activity as a percentage of the control cells. Values are expressed as means ± SD of two independent experiments; *p < 0.05 compared with control with Student's t-test. (B) Representative pictures of control and treated cells after invasion through matrigel-coated cell culture inserts.

and **16c** inhibited MDA-MB-231 cell migration and invasion at nontoxic concentrations of 0.08 and 0.4 μM, respectively. It should be mentioned that, at the indicated concentrations, also an inhibitory effect on cell proliferation was noted (Figure 10). In contrast, compound **9** did not inhibit migration or invasion of tumor cells at nontoxic concentrations.

Biological Stability of the Compounds. To investigate the biological stability of **9** and **16c**, both compounds were incubated in human serum or in mouse liver extract. The amount of intact compound (compared with the amount present at t = 0) was determined at different time points by HPLC analysis (Figure 11). Compound **16c** showed very good stability both in liver extract (Figure 11A, empty bars) and in human serum (Figure 11B, empty bars), with more than 90% and 70% of intact compound, respectively, after 3 h of incubation. However, the initial hit **9** proved to be rapidly degraded under both conditions as represented by the filled bars in Figure 11A,B. Thus, compound **16c** showed much better biological stability than **9**.

dx.doi.org/10.1021/jm401939g | J. Med. Chem. 2014, 57, 3924−3938

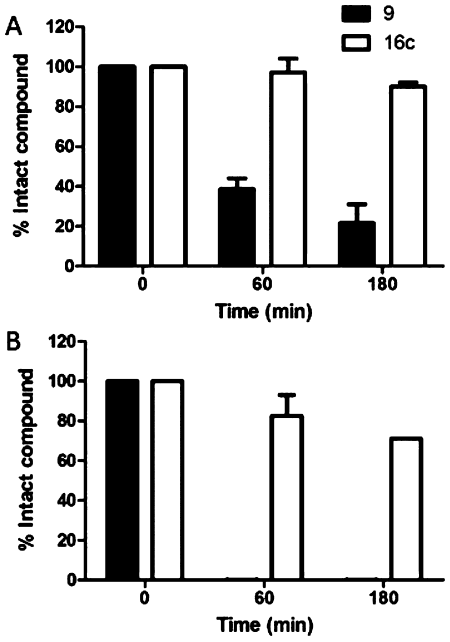

Figure 11. Stability of **9** and **16c** in the presence of mouse liver extract (A) or human serum (B). Compounds were incubated in 50% mouse liver extract (in PBS) (A) or in 10% human serum (in PBS) (B). The amount of intact compound (compared with the amount present at t = 0) was determined at different time points by HPLC analysis. Values are expressed as means ± SD of two independent experiments.

CONCLUSIONS

Compounds that target the α,β-tubulin dimer at the colchicine-binding site (or colchicine-like compounds) have been proposed as valuable anticancer agents since they combine antimitotic properties with vascular disrupting capacity. In an effort to identify new chemical entities with this profile, we have performed a ligand 3D shape virtual screening campaign using as queries compounds that target the α,β-tubulin dimer at the colchicine-binding site. Compound **9** (a cyclohexanedione derivative) was identified as a hit, based on its antiproliferative and tubulin binding (confirmed by MTC displacement) capacity. The synthesis and biological evaluation of structural analogues of compound **9** have allowed the identification of new derivatives with antiproliferative activities against endothelial and tumor cell lines in the submicromolar range, being 100-fold more potent than the initial hit. In particular, compound **16c** showed IC_{50} values of 0.09 μM against HMEC-1 and BAEC. Studies performed to determine the mechanism of action of this new series of compounds, employing **16c** as a representative example, revealed that they caused cell cycle arrest in G2/M phase and an increase in subG1 cells, undergoing apoptosis at 0.3 μM. Binding at the colchicine-binding site in tubulin was confirmed by a competition assay with *N,N′*-ethylenebis(iodoacetamide) and by fluorescence spectroscopy. Moreover, compound **16c** caused vascular disruption at 1 μM, as shown by its ability to destroy an established endothelial tubular network, and inhibited the migration and invasion of human breast carcinoma cells. The compound also proved stable in mouse liver extract and human serum. Thus, these tubulin-binding compounds represent a promising chemotype of antiproliferative and antivascular agents that should be further explored.

EXPERIMENTAL SECTION

Computational Methods. All VS calculations have been performed with a Dell Precision T7400 workstation. The software packages used for the VS (FILTER, OMEGA, ROCS, and VIDA) were obtained from OpenEye Scientific Software (www.eyesopen.com) by an academic license.

Database Preparation. The database compounds were obtained from the ZINC database,[19] version 8, and contained about 8.5 million compounds in SMILE string format.[20] The initial filter was performed with the "druglike filter" implemented in the tool FILTER v2.1.1 and only selected terms were customized from the default file, such as the allowed molecular weight (150−800), number of heavy atoms (9−60); ring size (7), number of carbon atoms (3−60), maximum number of hydrogen-bond donors and acceptors (10 and 11, respectively), and maximum xlogP (6.85). The filtered data set was thus reduced to 2.8 million compounds. 2D to 3D conversion and generation of conformational ensembles was carried out with OMEGA v2.3.2. This tool is controlled by a configuration file in which three parameters were changed as compared to the default values. The maximum number of output conformations of each molecule was set to 300, the energy window was set to 20 kcal/mol in order to discard high-energy conformations, and, finally, a RMSD cutoff of 0.75 Å was established below which two conformations were considered to be too similar. When submitted to OMEGA, a total of 510 million conformers (in mol2 format) were obtained and submitted to the VS protocol.

Virtual Screening with ROCS. ROCS v3.1.2 (Rapid Overlay of Chemical Structures) method was used for the virtual screening. ROCS overlays the multiconformer compound's database in shape and chemistry ("color) with respect to the reference ligand. As query molecules, the single conformation found in the α,β-tubulin−ligand X-ray structures of DAMA-colchicine (PDB ID 1sa0)[26] and TN-16 (PDB ID 3hkd)[27] were used. ROCS was run using the default settings. The output conformations of ROCS were ranked according to their shape similarity with the query using a Tanimoto coefficient of 0.75 and a ComboScore (shape plus color) of 1.4. Final results were visualized and analyzed with VIDA v4.1.1. When this protocol was applied using DAMA-colchicine as query, the scoring list showed structures too similar to colchicine, and this campaign was abandoned. VS carried out with TN-16 as query resulted in a total of 170 compounds that were clustered by visual inspection into nine chemical families. Only the best-ranked compound of each family was selected as a hit for the anti-proliferative assay, of which only six were available at the time and subsequently tested.

Chemistry Procedures. Melting points were obtained on a Reichert-Jung Kofler apparatus and are uncorrected. The elemental analysis was performed with a Heraeus CHN-O-RAPID instrument. The elemental compositions of the compounds agreed to within ±0.4% of the calculated values. For all the tested compounds, satisfactory elemental analysis was obtained, supporting >95% purity. Electrospray mass spectra were measured on a quadrupole mass spectrometer equipped with an electrospray source (Hewlett-Packard, LC/MS HP 1100). ^{1}H and ^{13}C NMR spectra were recorded on a Varian INNOVA 300 operating at 299 and 75 MHz, respectively, a Varian INNOVA-400 operating at 399 and 99 MHz, respectively, and a VARIAN SYSTEM-500 operating a 499 and 125 MHz, respectively.

Analytical TLC was performed on silica gel 60 F_{254} (Merck) precoated plates (0.2 mm). Spots were detected under UV light (254 nm) and/or charring with ninhydrin or phophomolibdic acid. Separations on silica gel were performed by preparative centrifugal circular thin-layer chromatography (CCTLC) on a Chromatotron [Kiesegel 60 PF_{254} gipshaltig (Merck)], with layer thickness of 1 and 2 mm and flow rate of 4 or 8 mL/min, respectively. Flash column chromatography was performed in a Biotage Horizon instrument.

Microwave reactions were performed using the Biotage Initiator 2.0 single-mode cavity instrument from Biotage (Uppsala, Sweden). Experiments were carried out in sealed microwave process vials utilizing the standard absorbance level (400 W maximum power). The

temperature was measured with an IR sensor on the outside of the reaction vessel.

The synthesis of the different series of compounds has been performed by applying the here described general procedures. A few key compounds are described in this Experimental Section. Full details and analytical and spectroscopic data for all the compounds are included in the Supporting Information.

5-Oxo-1,2,5,6-tetrahydro-[1,1′-biphenyl]-3-yl propionate (11). To a solution of 5-phenylcyclohexane-1,3-dione (300 mg, 1.59 mmol) and DMAP (59 mg, 0.48 mmol) in CH_2Cl_2 (1.6 mL) was added Hunig's base (DIPEA) (277 μL, 1.59 mmol). Then, propionyl chloride (147 μL, 1.59) was added dropwise and the reaction mixture was refluxed for 2 h. After cooling, HCl (1 N, 10 mL) was added, and the crude mixture was extracted with ethyl acetate (10 mL × 3). The organic layer was washed with brine (15 mL), dried over Na_2SO_4, concentrated, and purified by flash chromatography (hexane/ethyl acetate 3:1) to yield 250 mg (64%) of **11** as an oil. EM (ES, positive mode): m/z 245 $(M + H)^+$. ^{1}H NMR (DMSO-d_6, 500 MHz): δ 1.07 (t, 3H, J = 7.4 Hz, CH_3), 2.47 (dd, 1H, J = 16.6, 2.9 Hz, H-2), 2.57 (c, 2H, J = 7.5 Hz, CH_2), 2.73 (dd, 1H, J = 16.2, 12.9 Hz, H-2), 2.63 (dd, 1H, J = 17.7, 4.3 Hz, H-6), 2.87 (ddd, 1H, J = 17.6, 10.9, 2.0 Hz, H-6), 3.28 (m, 1H, H-1), 5.91 (d, 1H, J = 2.1 Hz, H-4), 7.24 (t, 1H, J = 7.0 Hz, 4-Ar), 7.35 (m, 4H, Ar).

5-Phenyl-2-propionylcyclohexane-1,3-dione (12). A microwave vial was charged with 5-phenylcyclohexane-1,3-dione (**10**) (500 mg, 2.66 mmol), propionyl chloride (490 μL, 5.31 mmol), anhydrous K_2CO_3 (809 mg, 5.85 mmol), 1,2,4-triazole (73 mg, 1.06 mmol), and tetrabutylammonium bromide (429 mg, 1.33 mmol) in anhydrous acetonitrile (10 mL). The reaction vessel was sealed, stirred under argon atmosphere for 10 min, and heated in a microwave reactor at 70 °C for 2 h. After cooling, the reaction mixture was acidified with 1 N HCl and the mixture was extracted with ethyl acetate. The organic layer was dried over Na_2SO_4, concentrated, and purified by flash chromatography (hexane/ethyl acetate) to yield 330 mg (51%) of **12** as a white solid. Mp: 71−73 °C. EM (ES, positive mode): m/z 245 $(M + H)^+$. ^{1}H NMR (DMSO-d_6, 300 MHz): δ (enol form) 1.05 (t, 3H, J = 7.3 Hz, CH_3), 2.62−2.71 (m, 2H, H-4, H-6), 2.87−2.95 (m, 2H, H-4, H-6), 3.01 (q, 2H, J = 7.2 Hz, CH_2), 3.46 (m, 1H, H-5), 7.23−7.38 (m, 5H, Ar). Although this compound was mentioned in ref 28, no analytical or spectroscopic data were provided.

General Procedure for the Reaction of 2-Acyl-5-phenylcyclohexane-1,3-diones with Anilines. A microwave vial was charged with 2-acyl-5-phenylcyclohexane-1,3-dione (1.0 mmol), the appropriate aniline (1.5 mmol), and 4 Å molecular sieves in toluene (2 mL). The reaction vessel was sealed and heated in a microwave reactor at 150 °C for 2 h. After cooling, the solvent was evaporated. The resulting residue was purified as specified.

*2-(1-((3-Hydroxyphenyl)amino)propylidene)-5-phenylcyclohexane-1,3-dione (**14a**).* Following the general procedure for the reaction of 2-acyl-5-phenylcyclohexane-1,3-diones with anilines, a microwave vial was charged with 5-phenyl-2-propionylcyclohexane-1,3-dione (**12**) (40 mg, 0.16 mmol) and 3-aminophenol (26 mg, 0.24 mmol) in toluene. The residue was worked up and purified by CCTLC in a Chromatotron (dichloromethane/methanol, 40:1) to yield 50 mg (93%) of **14a** as a white solid. Mp: 199−201 °C. EM (ES, positive mode): m/z 336 $(M + H)^+$. ^{1}H NMR (DMSO-d_6, 500 MHz): δ 1.06 (t, 3H, J = 7.3 Hz, CH_3), 2.60−2.64 (m, 2H, H-4, H-6), 2.80−2.89 (m, 4H, H-4, H-6, CH_2), 3.33 (m, 1H, H-5), 6.65 (t, 1H, J = 2.2 Hz, Ar), 6.70 (m, 1H, Ar), 6.81 (ddd, 1H, J = 8.2, 2.4, 0.9 Hz, Ar), 7.18−7.25 (m, 1H, Ar), 7.27 (t, 1H J = 8.0 Hz, Ar), 7.32 (d, 4H, J = 4.4 Hz, Ar), 9.90 (br s, 1H, OH), 14.94 (br s, 1H, NH). ^{13}C NMR (DMSO-d_6, 125 MHz): δ 12.8 (CH_3), 23.4 (CH_2), 36.0 (C-5), 46.0 (C-4, C-6), 106.7 (NHC=*C*), 112.9, 115.8, 116.4, 126.5, 126.7, 128.5, 130.4, 136.8, 143.4, 158.2 (Ar), 177.0 (NHC=C). Anal. Calcd for ($C_{21}H_{21}NO_3$): C, 75.20; H, 6.31; N, 4.18. Found: C, 75.33; H, 6.12; N, 4.36.

*2-(1-((4-Hydroxyphenyl)amino)propylidene)-5-phenylcyclohexane-1,3-dione (**14b**).* Following the general procedure for the reaction of 2-acyl-5-phenylcyclohexane-1,3-diones with anilines, a microwave vial was charged with 5-phenyl-2-propionylcyclohexane-1,3-dione (**12**) (40 mg, 0.16 mmol) and 4-aminophenol (26 mg, 0.24 mmol) in toluene. The residue was worked up and purified by CCTLC in a Chromatotron (dichloromethane/methanol 40:1) to yield 30 mg (56%) of **14b** as a white solid. Mp: 203−205 °C. EM (ES, positive mode): m/z 336 $(M + H)^+$. ^{1}H NMR (DMSO-d_6, 300 MHz): δ 1.02 (t, 3H, J = 7.3 Hz, CH_3), 2.59−2.63 (m, 2H, H-4, H-6), 2.78−2.88 (m, 4H, H-4, H-6, CH_2), 3.32 (m, 1H, H-5), 6.85 (m, 2H, Ar), 7.11 (m, 2H, Ar), 7.23 (m, 1H, Ar), 7.33 (d, 4H, J = 4.4 Hz, Ar), 9.81 (br s, 1H, OH), 14.73 (br s, 1H, NH). ^{13}C NMR (DMSO d_6, 100 MHz): δ 13.0 (CH_3), 23.7 (CH_2), 36.5 (C-5), 46.5 (C-4, C-6), 107.1 (NHC=*C*), 116.4, 127.0, 127.2, 127.3, 127.7, 128.9, 143.9, 157.5 (Ar), 178.0 (NH*C*=C). Anal. Calcd for ($C_{21}H_{21}NO_3$): C, 75.20; H, 6.31; N, 4.18. Found: C, 74.98; H, 6.13; N, 4.37.

*2-(1-((2-Methoxyphenyl)amino)propylidene)-5-phenylcyclohexane-1,3-dione (**14c**).* Following the general procedure for the reaction of 2-acyl-5-phenylcyclohexane-1,3-diones with anilines, a microwave vial was charged with 5-phenyl-2-propionylcyclohexane-1,3-dione (**12**) (35 mg, 0.14 mmol) and *o*-anisidine (24 μL, 0.21 mmol) in toluene. The residue was worked up and purified by CCTLC in a Chromatotron (hexane/ethyl acetate, 5:1) to yield 48 mg (98%) of **14c** as a white solid. Mp 93−95 °C. EM (ES, positive mode): m/z 350 $(M + H)^+$. ^{1}H NMR (DMSO-d_6, 400 MHz): δ 0.98 (t, 3H, J = 7.3 Hz, CH_3), 2.59−2.64 (m, 2H, H-4, H-6), 2.80−2.84 (m, 4H, H-4, H-6, CH_2), 3.36 (m, 1H, H-5), 3.82 (s, 3H, OCH_3), 7.06 (td, 1H, J = 7.6, 1.2 Hz, Ar), 7.19−7.27 (m, 2H, Ar), 7.30 (dd, 1H, J = 7.7, 1.5 Hz, Ar), 7.33 (d, 2H, J = 1.4 Hz, Ar), 7.34 (s, 2H, Ar), 7.39−7.46 (m, 1H, Ar), 14.69 (br s, 1H, NH). ^{13}C NMR (DMSO-d_6, 100 MHz): δ 12.2 (CH_3), 25.5 (CH_2), 36.0 (C-5), 46.1 (C-4, C-6), 55.8 (OCH_3), 106.9 (NHC=*C*), 112.4, 120.7, 124.2, 126.5, 126.7, 127.5, 128.5, 129.7, 143.5, 153.5 (Ar), 178.0 (NH*C*=C). Anal. Calcd for ($C_{22}H_{23}NO_3$): C, 75.62; H, 6.63; N, 4.01. Found: C, 75.48; H, 6.52; N, 4.00.

Details of the synthesis and analytical and spectroscopic data for compounds **14d−j** are provided in the Supporting Information.

*2-Butyryl-5-phenylcyclohexane-1,3-dione (**15a**).* Following the described procedure for the synthesis of **12**, a microwave vial was charged with 5-phenylcyclohexane-1,3-dione (**10**) (500 mg, 2.66 mmol), butyryl chloride (548 μL, 5.31 mmol), anhydrous K_2CO_3 (809 mg, 5.85 mmol), 1,2,4-triazole (73 mg, 1.06 mmol), and tetrabutylammonium bromide (429 mg, 1.33 mmol) in anhydrous acetonitrile (10 mL) to yield 200 mg (29%) of **15a** as a white solid. Mp: 68−70 °C. EM (ES, positive mode): m/z 259 $(M + H)^+$. ^{1}H NMR (DMSO-d_6, 300 MHz): δ (enol form) 0.92 (t, 3H, J = 7.3 Hz, CH_3), 1.58 (m, 2H, CH_2), 2.69 (m, 2H, H-4, H-6), 2.92 (m, 2H, H-4, H-6), 2.97 (t, 2H, J = 7.4 Hz, CH_2), 3.37−3.45 (m, 1H, H-5), 7.25 (m, 1H Ar), 7.33 (m, 4H, Ar). Note: Although this compound was mentioned in ref 29, no analytical data were provided.

*2-Acetyl-5-phenylcyclohexane-1,3-dione (**15b**).* Following the described procedure for the synthesis of **12**, a microwave vial was charged with 5-phenylcyclohexane-1,3-dione (**10**) (500 mg, 2.66 mmol), acetyl chloride (417 μL, 5.31 mmol), anhydrous K_2CO_3 (809 mg, 5.85 mmol), 1,2,4-triazole (73 mg, 1.06 mmol), and tetrabutylammonium bromide (429 mg, 1.33 mmol) in anhydrous acetonitrile (10 mL) to yield 350 mg (54%) of **15b** as a white solid. Mp: 100−102 °C. EM (ES, positive mode): m/z 231 $(M + H)^+$. ^{1}H NMR (DMSO-d_6, 300 MHz): δ (enol form) 2.55 (s, 3H, CH_3), 2.66−2.72 (m, 2H, H-4, H-6), 2.94 (m, 2H, H-4, H-6), 3.36−3.47 (m, 1H, H-5), 7.22−7.34 (m, 5H, Ar). Note: Although this compound was mentioned in ref 29, no analytical data were provided.

*2-(1-((2-Methoxyphenyl)amino)butylidene)-5-phenylcyclohexane-1,3-dione (**16a**).* A mixture of 2-butyryl-5-phenylcyclohexane-1,3-dione (**15a**) (60 mg, 0.23 mmol) and *o*-anisidine (30 μL, 0.22 mmol) in 1.5 mL of toluene was heated for 2 days under reflux in a flask equipped with a Dean−Stark trap. Volatiles were removed, and the crude reaction mixture was purified by CCTLC in a Chromatotron (hexane/ethyl acetate, 5:1) to yield 70 mg (84%) of **16a** as a pale yelow solid. Mp: 108−110 °C. EM (ES, positive mode): m/z 364 $(M + H)^+$. ^{1}H NMR (DMSO-d_6, 400 MHz): δ 0.74 (t, 3H, J = 7.3 Hz, CH_3), 1.40 (m, 2H, CH_2), 2.59−2.63 (m, 2H, H-4, H-6), 2.77 (m, 4H, H-4, H-6, CH_2), 3.29−3.37 (m, 1H, H-5), 3.82 (s, 3H, OCH_3), 7.05 (m, 1H, J = 7.6, 1.2 Hz, Ar), 7.21 (dd, 1H, J = 8.4, 1.2 Hz, Ar), 7.25 (m, 1H, Ar), 7.28 (dd, 1H, J = 7.7, 1.6 Hz, Ar), 7.33 (d, 2H, J = 1.3 Hz,

dx.doi.org/10.1021/jm401939g | J. Med. Chem. 2014, 57, 3924−3938

Ar), 7.33 (s, 2H, Ar), 7.42 (ddd, 1H, J = 8.6, 7.6, 1.6 Hz, Ar), 14.73 (br s, 1H, NH). ^{13}C NMR (DMSO-d_6, 100 MHz): δ 14.1 (CH_3), 21.3 (CH_2), 31.9 (CH_2), 36.0 (C-5), 46.0, 46.5 (C-4, C-6), 55.8 (OCH_3), 107.2 (NHC=*C*), 112.3, 120.7, 124.4, 126.5, 126.5, 127.5, 128.5, 129.6, 143.4, 153.5 (Ar), 176.4 (NHC=C). Anal. Calcd for ($C_{23}H_{25}NO_3$): C, 76.01; H, 6.93; N, 3.85. Found: C, 75.93; H, 6.68; N, 4.10.

*5-Phenyl-2-(1-(o-tolylamino)butylidene)cyclohexane-1,3-dione (**16b**).* Following the general procedure for the reaction of 2-acyl-5-phenylcyclohexane-1,3-diones with anilines, a microwave vial was charged with 2-butyryl-5-phenylcyclohexane-1,3-dione (**15a**) (30 mg, 0.12 mmol) and *o*-toluidine (18 μL, 0.17 mmol) in toluene. The residue was worked up and purified by CCTLC in a Chromatotron (hexane/ethyl acetate, 5:1) to yield 42 mg (99%) of **16b** as a white solid. Mp: 98−100 °C. EM (ES, positive mode): m/z 348 (M + H)$^+$. ^{1}H NMR (DMSO-d_6, 500 MHz): δ 0.74 (t, 3H, J = 7.3 Hz, CH_3), 1.40 (m, 2H, CH_2), 2.17 (s, 3H, CH_3), 2.63 (dd, 2H, J = 16.7, 3.7 Hz, H-4, H-6), 2.75 (t, 2H, J = 7.3 Hz, CH_2), 2.85 (m, 2H, H-4, H-6), 3.32−3.39 (m, 1H, H-5), 7.22−7.26 (m, 1 H, Ar), 7.27 (dd, 1H, J = 7.2, 2.1 Hz, Ar), 7.34 (m, 6H, Ar), 7.41 (m, 1H, Ar), 14.91 (br s, 1H, NH). ^{13}C NMR (DMSO-d_6, 125 MHz): δ 14.2 (CH_3), 17.5 (CH_3), 21.3 (CH_2), 31.8 (CH_2), 36.0 (C-5), 46.0 (C-4, C-6), 107.0 (NHC=*C*), 126.5, 126.7, 126.8, 126.9, 128.3, 128.5, 131.0, 133.6, 135.0, 143.5 (Ar), 176.1 (NHC=C). Anal. Calcd for ($C_{23}H_{25}NO_2$): C, 79.51; H, 7.25; N, 4.03. Found: C, 79.27; H, 6.98; N, 4.11.

*2-(1-((2-Methoxyphenyl)amino)ethylidene)-5-phenylcyclohexane-1,3-dione (**16c**).* Following the general procedure for the reaction of 2-acyl-5-phenylcyclohexane-1,3-diones with anilines, a microwave vial was charged with 2-acetyl-5-phenylcyclohexane-1,3-dione (**15b**) (40 mg, 0.17 mmol) and *o*-anisidine (30 μL, 0.26 mmol) in toluene. The residue was worked up and purified by CCTLC in a Chromatotron (hexane/ethyl acetate, 5:1) to yield 49 mg (86%) of **16c** as a white solid. Mp: 139−141 °C. EM (ES, positive mode): m/z 336 (M + H)$^+$. ^{1}H NMR (DMSO-d_6, 500 MHz): δ 2.41 (s, 3H, CH_3), 2.60−2.63 (m, 2H, H-4, H-6), 2.82 (m, 2H, H-4, H-6), 3.36 (m, 1H, H-5), 3.84 (s, 3H, OCH_3), 7.04 (td, 1H, J = 7.6, 1.2 Hz, Ar), 7.20 (dd, 1 H, J = 8.5, 1.2 Hz, Ar), 7.21−7.26 (m, 1H, Ar), 7.32 (dd, 1H, J = 7.8, 1.6 Hz, Ar), 7.33 (d, 2H, J = 0.8 Hz, Ar), 7.34 (s, 2H, Ar), 7.39 (m, 1H, Ar), 14.78 (br s, 1H, NH). ^{13}C NMR (DMSO-d_6, 125 MHz): δ 19.7 (CH_3), 36.1 (C-5), 46.4 (C-4, C-6), 55.8 (OCH_3), 108.4 (NHC=*C*), 112.3, 120.6, 124.5, 126.5, 126.7, 128.9, 128.5, 129.2, 143.5, 153.1 (Ar), 172.4 (NHC=C). Anal. Calcd for ($C_{21}H_{21}NO_3$): C, 75.20; H, 6.31; N, 4.31. Found: C, 74.98; H, 6.32; N, 4.20.

*5-Phenyl-2-(1-(o-tolylamino)ethylidene)cyclohexane-1,3-dione (**16d**).* Following the general procedure for the reaction of 2-acyl-5-phenylcyclohexane-1,3-diones with anilines, a microwave vial was charged with 2-acetyl-5-phenylcyclohexae-1,3-dione (**15b**) (30 mg, 0.13 mmol) and *o*-toluidine (22 μL, 0.20 mmol) in toluene. The residue was worked up and purified by CCTLC in a Chromatotron (hexane/ethyl acetate, 5:1) to yield 25 mg (60%) of **16d** as a white solid. Mp: 128−130 °C. EM (ES, positive mode): m/z 320 (M + H)$^+$. ^{1}H NMR (DMSO-d_6, 300 MHz): δ 2.20 (s, 3H, CH_3), 2.38 (s, 3H, CH_3), 2.59−2.66 (m, 2H, H-4, H-6), 2.79−2.89 (m, 2H, H-4, H-6), 3.36 (m, 1H, H-5), 7.23−7.40 (m, 9H, Ar), 14.91 (br s, 1H, NH). ^{13}C NMR (DMSO-d_6, 100 MHz): δ 17.4 (CH_3), 19.6 (CH_3), 36.1 (C-5), 45.8 (C-4, C-6), 108.2 (NHC=*C*), 126.5, 126.7, 126.9, 128.1, 128.49, 131.0, 133.3, 135.1, 143.5, 159.9 (Ar), 172.7 (NHC=C). Anal. Calcd for ($C_{21}H_{21}NO_2$): C, 78.97; H, 6.63; N, 4.39. Found: C, 78.69; H, 6.54; N, 4.27.

Biological Methods. In all these assays, colchicine has been used as a reference compound.

Cell Proliferation. Endothelial Cells. Mouse brain endothelial cells (MBEC), bovine aortic endothelial cells (BAEC), and human dermal microvascular endothelial cells (HMEC-1) were seeded in 48-well plates at 10 000 cells/well (except HMEC-1 at 20,000/well). After 24 h, 5-fold dilutions of the compounds were added. The cells were allowed to proliferate 3 days (or 4 days for HMEC-1) in the presence of the compounds, trypsinized, and counted by means of a Coulter counter (Analis, Belgium).

Tumor Cells. Human cervical carcinoma (HeLa) cells were seeded in 96-well plates at 15 000 cells/well in the presence of different concentrations of the compounds. After 4 days of incubation, the cells were trypsinized and counted in a Coulter counter. Suspension cells (Mouse leukemia L1210 and human lymphoid Cem cells) were seeded in 96-well plates at 60 000 cells/well in the presence of different concentrations of the compounds. L1210 and Cem cells were allowed to proliferate for 48 or 96 h, respectively, and then counted in a Coulter counter. The 50% inhibitory concentration (IC_{50}) was defined as the compound concentration required to reduce cell proliferation by 50%.

Cell Cycle Analysis. HMEC-1 cells were seeded in 6-well plates at 125 000 cells/well in DMEM with 10% FCS. After 24 h, the cells were exposed to different concentrations of the compounds. After 24 h, the DNA of the cells was stained with propidium iodide using the CycleTEST PLUS DNA Reagent Kit (BD Biosciences, San Jose, CA). The DNA content of the stained cells was assessed by flow cytometry on a FACSCalibur flow cytometer and analyzed with CellQuest software (BD Biosciences) within 3 h after staining. Cell debris and clumps were excluded from the analysis by appropriate dot plot gating. Percentages of sub-G1, G1, S, and G_2/M cells were estimated using appropriate region markers.[35]

Tube Formation. Wells of a 96-well plate were coated with 70 μL of matrigel (10 mg/mL, BD Biosciences, Heidelberg, Germany) at 4 °C. After gelatinization at 37 °C during 30 min, HMEC-1 cells were seeded at 60 000 cells/well on top of the matrigel in 200 μL of DMEM containing 10% FCS. After 3 h of incubation at 37 °C, when the endothelial cells had reorganized to form tubelike structures, the compounds were added. Ninety minutes later, colchicine, which was added as a reference compound, had destroyed the endothelial tubes. The cultures were photographed at 100× magnification.

Tubulin Binding. Human breast carcinoma MDA-MB-231 cells were seeded in 6-well plates at 500 000 cells/well. After 48 h, compounds were added to the cells for 16 h before adding EBI (*N,N′*-ethylenebis(iodoacetamide) at 100 μM. After 1.5 h, the cells were harvested and cell extracts were prepared for Western blot analysis. Twenty micrograms of proteins was subjected to gel electrophoresis using 0.1% SDS (85% purity) and 10% polyacrylamide gels. After electrophoresis, proteins were transferred to pretreated Hybond-P polyvinylidene difluoride (PVDF) membranes (Amersham Biosciences). The membranes were incubated for 1 h at room temperature in blocking buffer (2.5% nonfat dry milk in PBS containing 0.1% Tween) and subsequently for 16 h at 4 °C in blocking buffer with primary antibodies raised against β-tubulin. After washing, the membranes were incubated with the corresponding horseradish peroxidase-conjugated secondary antibody in blocking buffer for 25 min at room temperature. Next, the membranes were washed extensively. Immunoreactive proteins were detected by chemiluminescence (ECLplus, Bio-Rad).

In living cells, EBI cross-links the cysteine residues at positions 239 and 354 of β-tubulin. This β-tubulin adduct formed by EBI is easily detectable by Western blot as a second immunoreactive band that migrates faster than β-tubulin.

Transwell Migration and Invasion Assays. Migration and invasion of MDA-MB-231 cells were evaluated using inserts with 8 μm pore size (BD Biosciences). For tumor cell invasion, the insets were coated with 10% matrigel (BD Biosciences) for 1 h at 37 °C. MDA-MB-231 cells were trypsinized and counted. Cells (5×10^4) were seeded in the upper chamber in DMEM containing 1% FBS and the test compound. The cells were allowed to migrate for 15 h through the inserts using 10% FBS as chemoattractant. Next, the nonmigrating cells were removed; the cells that reached the lower surface of the membrane were photographed and counted.

To measure the effects of the compounds on MDA-MB-231 cell growth during the course of the migration and invasion experiments, 5×10^4 cells were seeded in 96-well plates in the presence of different concentrations of the compounds. After 17 h, the cells were trypsinized and counted.

Stability of the Compounds. The test compounds (**9** and **16c**) were exposed at 100 μM in 5% DMSO to concentrated mouse liver

extract (50% in PBS in a final volume of 200 μL) or to human serum (10% in PBS in a final volume of 300 μL) and incubated for 60 and 180 min at 37 °C. Next, 50 μL of the reaction mixture was withdrawn and added to 100 μL of ice-cold methanol for another 10 min. Then, the mixtures were centrifuged for 10 min at 10 000 rpm, and the supernatants were evaporated in a Speedvac apparatus (Savant, Werchter, Belgium). The dried residue was resolubilized in PBS and analyzed on a C18 reverse-phase column (LiChroCard, Merck, Darmstadt, Germany) by HPLC (Waters, Milford, MA) using a gradient system of water/acetonitrile (50%). Compound detection was performed at 305 nm.

Determination of Binding Constants. Proteins and Ligands. Calf brain tubulin was purified as described.[49] 2-Methoxy-5-(2,3,4-trimethoxyphenyl)-2,4,6-cycloheptatrien-1-one (MTC)[50] was a kind gift of Prof. T. J. Fitzgerald (School of Pharmacy, Florida A & M University, Tallahassee, FL). (*R*)-(+)-Ethyl 5-amino-2-methyl-1,2-dihydro-3-phenylpyrido[3,4-*b*]pyrazin-7-ylcarbamate (R-PT)[51] was a kind gift of Prof. G. A. Rener (Organic Chemistry Research Department, Southern Research Institute, Birmingham, AL). The compounds were diluted in 99.8% DMSO-d_6 (Merck, Darmstadt, Germany) to a final concentration of 10 mM and stored at −80 °C.

Determination of Binding Constants. Competition of the compounds with MTC was tested by the change in the intensity of fluorescence of MTC upon binding to tubulin. The fluorescence emission spectra (excitation at 350 nm) of 10 μM tubulin and 10 μM MTC in 10 mM sodium phosphate, 0.1 mM GTP, pH 7.0, were measured in the presence or the absence of 20 μM of the desired ligand with 5 nm excitation and emission slits using a Jobin-Ybon SPEX Fluoromax-2 (HORIBA, Ltd., Kyoto, Japan). The decrease in the intensity of the fluorescence in the presence of the competitor ligand indicated competition for the same binding site.

The binding constant of R-PT for dimeric tubulin was determined using the competition method in 10 mM sodium phosphate, 0.1 mM GTP, pH 7.0, at 25 °C. To do so 0.2 μM of R-PT was incubated with increasing amounts of tubulin up to 10 μM and, vice versa, 0.2 μM of tubulin was incubated with increasing amounts of R-PT up to 10 μM, and the fluorescence emission spectra (excitation 374 nm) of the samples (5 nm excitation and emission slits) were determined using a Jobin-Ybon SPEX Fluoromax-2 (HORIBA, Ltd., Kyoto, Japan). Using these spectra it is possible to calculate the free and the bound R-PT concentration for each sample and thus to determine the binding constant of R-PT for tubulin.

Once the K_b of R-PT is determined (5.1×10^6 M^{-1}) this compound could be used as a reference ligand. For that purpose, the fluorescence emission of a previous mixed sample of 0.2 μM R-PT and 0.2 μM tubulin was evaluated in the presence of increasing concentrations of studied ligand in a black 96-well plate (0, 0.05, 0.2, 0.5, 2, 5, 10, 30, 50, 70 μM). The samples were incubated for 30 min at 25 °C in a Varioskan plate reader (Thermo Scientific, Waltham, MA) before the fluorescence emission intensity at 456 nm (excitation 374 nm) was measured. The data were analyzed and the binding constants determined using Equigra V5.0.[42]

Immunocytochemistry. MDA-MB-231 cells were grown on poly-L-lysine-precoated 8-well chamber slides (Lab-Tek, Nunc, Roskilde, Denmark) in DMEM containing 10% FBS and exposed to compound (DMSO, **16c**, or colchicine). After 8 h, the cells were fixed in 4% PFA for 15 min at room temperature, washed three times with PBS and permeabilized for 10 min at room temperature with 0.25% Triton X-100 (Sigma-Aldrich). Nonspecific binding sites were blocked for 30 min at room temperature with 0.5% BSA in PBS. The cells were then incubated with a monoclonal anti-β-tubulin antibody (2 μg/mL, Sigma-Aldrich) for 2 h at room temperature, washed three times, and incubated for 1 h at room temperature with goat anti-mouse Alexa Fluor 488 (4 μg/mL; Molecular Probes, Invitrogen) in 0.5% BSA. After three washes, nuclei were stained with 300 nM 4′,6-diamidino-2-phenylindole (DAPI) (Sigma-Aldrich). Fluorescent microscopic analysis was done with an Axiovert 200 M inverted microscope (Zeiss, Göttingen, Germany), using an EC Plan-Neofluar 40×/1.30 oil objective. Pictures were taken with an AxioCamMRm camera and processed with AxioVision Release 4.6 software (Zeiss).

■ ASSOCIATED CONTENT

Supporting Information

The synthesis and spectroscopic data of all the synthesized compounds are included, molecular structures (SMILES strings) of the virtual screening hits tested are included in Table S1, antiproliferative activity of the VS hits in endothelial and tumor cell lines is included in Table S2, dose−response curves of **9** in endothelial and tumor cell lines are included as Figure S2, and fluorescence emission spectra for the displacement of MTC by **9** and R-PT and MTC by **16c** are included as Figures S1 and S3, respectively. This material is available free of charge via the Internet at http://pubs.acs.org.

■ AUTHOR INFORMATION

Corresponding Authors

*S.L.: address, Rega Institute for Medical Research, Minderbroedersstraat 10, blok x-bus 1030, B-3000 Leuven, Belgium; phone, +32 (0) 16337355; fax, +32 (0) 16337340; e-mail, sandra.liekens@rega.kuleuven.be.

*E.-M.P.: address, Instituto de Química Médica (CSIC) Juan de la Cierva 3, 28006 Madrid, Spain; phone, +34 91 5680040; fax, 34 91 5644853; e-mail, empriego@iqm.csic.es.

Notes

The authors declare no competing financial interest.

■ ACKNOWLEDGMENTS

M.-D.C. thanks the Fondo Social Europeo (FSE) and the JAE Predoc Programme for a predoctoral fellowship. This work has received the ALMIRALL S.A award for young researchers (to M.-D.C) in the XVI call sponsored by the Spanish Society of Medicinal Chemistry (SEQT). This project has been supported by the Spanish Plan Nacional (SAF2009-13914-C02-01 and SAF2012-39760-C02-01 to M-J. C, M-J.P.-P., and E.-M.P.), Comunidad de Madrid (BIPEDD2; ref P2010/BMD-2457 to M.-J.C. and J.F.D.), the BIO2010-16351 (to J.F.D.) project from the Ministry of Economy and Competitiveness of Spain, and a FPI grant to G.S-C. We also wish to thank Eef Meyen, Lizzete van Berckelaer, and Ria Van Berwaer for excellent technical assistance. The authors thank Dr. José M. Andreu for fruitful discussions. We are grateful to OpenEye Scientific Software, Inc. for providing us with an academic license for their software. We are indebted to Matadero Vicente de Lucas de Segovia for providing calf brains for the tubulin purification.

■ ABBREVIATIONS USED

VDA, vascular-disrupting agent; VS, virtual screening; ROCS, rapid overlay of chemical structures; MTC, 2-methoxy-5-(2,3,4-trimethoxyphenyl)-2,4,6-cycloheptatrien-1-one; R-PT, (*R*)-(+)-ethyl 5-amino-2-methyl-1,2-dihydro-3-phenylpyrido[3,4-*b*]pyrazin-7-ylcarbamate.; EBI, *N*,*N*′-ethylene-bis-(iodoacetamide).

■ REFERENCES

(1) Folkman, J.; Bach, M.; Rowe, J. W.; Davidoff, F.; Lambert, P.; Hirsch, C.; Goldberg, A.; Hiatt, H. H.; Glass, J.; Henshaw, E. Tumor angionesis—Therapeutic implications. *N. Engl. J. Med.* **1971**, *285*, 1182−1186.

(2) (a) Roodink, I.; Leenders, W. P. J. Targeted therapies of cancer. Angiogenesis inhibition seems not enough. *Cancer Lett.* **2010**, *299*, 1−10. (b) Siemann, D. W.; Bibby, M. C.; Dark, G. G.; Dicker, A. P.; Eskens, F.; Horsman, M. R.; Marme, D.; LoRusso, P. M. Differentiation and definition of vascular-targeted therapies. *Clin. Cancer Res.* **2005**, *11*, 416−420.

(3) Potente, M.; Gerhardt, H.; Carmeliet, P. Basic and therapeutic aspects of angiogenesis. *Cell* **2011**, *146*, 873−887.
(4) McKeage, M. J.; Baguley, B. C. Disrupting established tumor blood vessels. An emerging therapeutic strategy for cancer. *Cancer* **2010**, *116*, 1859−1871.
(5) Mita, M. M.; Sargsyan, L.; Mita, A. C.; Spear, M. Vascular-disrupting agents in oncology. *Expert. Opin. Invest. Drugs* **2013**, *22*, 317−328.
(6) Denekamp, J. Endothelial cell proliferation as a novel approach to targeting tumor therapy. *Br. J. Cancer* **1982**, *45*, 136−139.
(7) Siemann, D. W. The unique characteristics of tumor vasculature and preclinical evidence for its selective disruption by tumor-vascular disrupting agents. *Cancer Treat. Rev.* **2011**, *37*, 63−74.
(8) (a) Konerding, M. A.; Fait, E.; Gaumann, A. 3D microvascular architecture of pre-cancerous lesions and invasive carcinomas of the colon. *Br. J. Cancer* **2001**, *84*, 1354−1362. (b) Kakolyris, S.; Fox, S. B.; Koukourakis, M.; Giatromanolaki, A.; Brown, N.; Leek, R. D.; Taylor, M.; Leigh, I. M.; Gatter, K. C.; Harris, A. L. Relationship of vascular maturation in breast cancer blood vessels to vascular density and metastasis, assessed by expression of a novel basement membrane component, LH39. *Br. J. Cancer* **2000**, *82*, 844−851.
(9) Spear, M. A.; LoRusso, P.; Mita, A.; Mita, M. Vascular disrupting agents (VDA) in oncology: Advancing towards new therapeutic paradigms in the clinic. *Curr. Drug Targets* **2011**, *12*, 2009−2015.
(10) Lu, Y.; Chen, J.; Xiao, M.; Li, W.; Miller, D. D. An overview of tubulin inhibitors that interact with the colchicine binding site. *Pharm. Res.* **2012**, *29*, 2943−2971.
(11) Galbraith, S. M.; Chaplin, D. J.; Lee, F.; Stratford, M. R. L.; Locke, R. J.; Vojnovic, B.; Tozer, G. M. Effects of combretastatin A4 phosphate on endothelial cell morphology in vitro and relationship to tumour vascular targeting activity in vivo. *Anticancer Res.* **2001**, *21*, 93−102.
(12) Tozer, G. M.; Kanthou, C.; Baguley, B. C. Disrupting tumour blood vessels. *Nat. Rev. Cancer* **2005**, *5*, 423−435.
(13) (a) Kanthou, C.; Tozer, G. M. The tumor vascular targeting agent combretastatin A-4-phosphate induces reorganization of the actin cytoskeleton and early membrane blebbing in human endothelial cells. *Blood* **2002**, *99*, 2060−2069. (b) Davis, P. D.; Dougherty, G. J.; Blakey, D. C.; Galbraith, S. M.; Tozer, G. M.; Holder, A. L.; Naylor, M. A.; Nolan, J.; Stratford, M. R. L.; Chaplin, D. J.; Hill, S. A. ZD6126: A novel vascular-targeting agent that causes selective destruction of tumor vasculature. *Cancer Res.* **2002**, *62*, 7247−7253. (c) Hori, K.; Saito, S. Microvascular mechanisms by which the combretastatin A-4 derivative AC7700 (AVE8062) induces tumour blood flow stasis. *Br. J. Cancer* **2003**, *89*, 1334−1344.
(14) (a) Jordan, M. A.; Wilson, L. Microtubules as a target for anticancer drugs. *Nat. Rev. Cancer* **2004**, *4*, 253−265. (b) Kanthou, C.; Tozer, G. M. Microtubule depolymerizing vascular disrupting agents: Novel therapeutic agents for oncology and other pathologies. *Int. J. Exp. Pathol.* **2009**, *90*, 284−294.
(15) Finkelstein, Y.; Aks, S. E.; Hutson, J. R.; Juurlink, D. N.; Nguyen, P.; Dubnov-Raz, G.; Pollak, U.; Koren, G.; Bentur, Y. Colchicine poisoning: The dark side of an ancient drug. *Clin. Toxicol.* **2010**, *48*, 407−414.
(16) (a) Young, S. L.; Chaplin, D. J. Combretastatin A4 phosphate: Background and current clinical status. *Expert. Opin. Invest. Drugs* **2004**, *13*, 1171−1182. (b) Kirwan, I. G.; Loadman, P. M.; Swaine, D. J.; Anthoney, D. A.; Pettit, G. R.; Lippert, J. W.; Shnyder, S. D.; Cooper, P. A.; Bibby, M. C. Comparative preclinical pharmacokinetic and metabolic studies of the combretastatin prodrugs combretastatin A4 phosphate and A1 phosphate. *Clin. Cancer Res.* **2004**, *10*, 1446−1453.
(17) Ripphausen, P.; Nisius, B.; Bajorath, J. State-of-the-art in ligand-based virtual screening. *Drug Discovery Today* **2011**, *16*, 372−376.
(18) (a) Nicholls, A.; McGaughey, G. B.; Sheridan, R. P.; Good, A. C.; Warren, G.; Mathieu, M.; Muchmore, S. W.; Brown, S. P.; Grant, J. A.; Haigh, J. A.; Nevins, N.; Jain, A. N.; Kelley, B. Molecular shape and medicinal chemistry: A perspective. *J. Med. Chem.* **2010**, *53*, 3862−3886. (b) Mohammed, M. Z.; Vyjayanti, V. N.; Laughton, C. A.; Dekker, L. V.; Fischer, P. M.; Wilson, D. M.; Abbotts, R.; Shah, S.; Patel, P. M.; Hickson, I. D.; Madhusudan, S. Development and evaluation of human AP endonuclease inhibitors in melanoma and glioma cell lines. *Br. J. Cancer* **2011**, *104*, 653−663.
(19) Irwin, J. J.; Sterling, T.; Mysinger, M. M.; Bolstad, E. S.; Coleman, R. G. ZINC: A free tool to discover chemistry for biology. *J. Chem. Inf. Model.* **2012**, *52*, 1757−1768.
(20) Weininger, D. SMILES, a chemical language and information system. 1. Introduction to methodology and encoding rules. *J. Chem. Inf. Comput. Sci.* **1988**, *28*, 31−36.
(21) FILTER; OpenEye Scientific Software Inc., Santa Fe, NM; www.eyesopen.com.
(22) OMEGA; OpenEye Scientific Software Inc., Santa Fe, NM; www.eyesopen.com.
(23) ROCS; OpenEye Scientific Software Inc., Santa Fe, NM; www.eyesopen.com.
(24) Grant, J. A.; Gallardo, M. A.; Pickup, B. T. A fast method of molecular shape comparison: A simple application of a Gaussian description of molecular shape. *J. Comput. Chem.* **1996**, *17*, 1653−1666.
(25) Rush, T. S.; Grant, J. A.; Mosyak, L.; Nicholls, A. A shape-based 3-D scaffold hopping method and its application to a bacterial protein−protein interaction. *J. Med. Chem.* **2005**, *48*, 1489−1495.
(26) Ravelli, R. B. G.; Gigant, B.; Curmi, P. A.; Jourdain, I.; Lachkar, S.; Sobel, A.; Knossow, M. Insight into tubulin regulation from a complex with colchicine and a stathmin-like domain. *Nature* **2004**, *428*, 198−202.
(27) Dorleans, A.; Gigant, B.; Ravelli, R. B. G.; Mailliet, P.; Mikol, V.; Knossow, M. Variations in the colchicine-binding domain provide insight into the structural switch of tubulin. *Proc. Natl. Acad. Sci. U. S. A.* **2009**, *106*, 13775−13779.
(28) Huang, K. H.; Veal, J. M.; Fadden, R. P.; Rice, J. W.; Eaves, J.; Strachan, J.-P.; Barabasz, A. F.; Foley, B. E.; Barta, T. E.; Ma, W.; Silinski, M. A.; Hu, M.; Partridge, J. M.; Scott, A.; DuBois, L. G.; Freed, T.; Steed, P. M.; Ommen, A. J.; Smith, E. D.; Hughes, P. F.; Woodward, A. R.; Hanson, G. J.; McCall, W. S.; Markworth, C. J.; Hinkley, L.; Jenks, M.; Geng, L.; Lewis, M.; Otto, J.; Pronk, B.; Verleysen, K.; Hall, S. E. Discovery of novel 2-aminobenzamide inhibitors of heat shock protein 90 as potent, selective and orally active antitumor agents. *J. Med. Chem.* **2009**, *52*, 4288−4305.
(29) Brown, S. M.; Bentley, T. W.; Jones, R. O. Process for the preparation of acylated cyclic 1,3-dicarbonyl compounds. WO 99/28282.
(30) Barker, J. J.; Barker, O.; Boggio, R.; Chauhan, V.; Cheng, R. K. Y.; Corden, V.; Courtney, S. M.; Edwards, N.; Falque, V. M.; Fusar, F.; Gardiner, M.; Hamelin, E. M. N.; Hesterkamp, T.; Ichihara, O.; Jones, R. S.; Mather, O.; Mercurio, C.; Minucci, S.; Montalbetti, C.; Muller, A.; Patel, D.; Phillips, B. G.; Varasi, M.; Whittaker, M.; Winkler, D.; Yarnold, C. J. Fragment-based identification of hsp90 inhibitors. *ChemMedChem.* **2009**, *4*, 963−966.
(31) Donkor, I. O.; Li, H.; Queener, S. F. Synthesis and DHFR inhibitory activity of a series of 6-substituted-2,4-diaminothieno 2,3-d pyrimidines. *Eur. J. Med. Chem.* **2003**, *38*, 605−611.
(32) Tamura, Y.; Yoshimoto, Y.; Kunimoto, K.; Tada, S.; Tomita, T.; Wada, T.; Seto, E.; Murayama, M.; Shibata, Y.; Nomura, A.; Ohata, K. Nonsteroidal antiinflamatory agents. 1. 5-Alkoxy-3-biphenylylacetic acids and related compounds as new potential antiinflamatory agents. *J. Med. Chem.* **1977**, *20*, 709−714.
(33) Zhang, W.; Benmohamed, R.; Arvanites, A. C.; Morimoto, R. I.; Ferrante, R. J.; Kirsch, D. R.; Silverman, R. B. Cyclohexane 1,3-diones and their inhibition of mutant SOD1-dependent protein aggregation and toxicity in PC12 cells. *Biorg. Med. Chem.* **2012**, *20*, 1029−1045.
(34) Ilic, M.; Ilas, J.; Dunkel, P.; Matyus, P.; Bohac, A.; Liekens, S.; Kikelj, D. Novel 1,4-benzoxazine and 1,4-benzodioxine inhibitors of angiogenesis. *Eur. J. Med. Chem.* **2012**, *58*, 160−170.
(35) Liekens, S.; Gijsbers, S.; Vanstreels, E.; Daelemans, D.; De Clercq, E.; Hatse, S. The nucleotide analog cidofovir suppresses basic fibroblast growth factor (FGF2) expression and signaling and induces

apoptosis in FGF2-overexpressing endothelial cells. *Mol. Pharmacol.* **2007**, *71*, 695−703.
(36) Fortin, S.; Lacroix, J.; Cote, M.-F.; Moreau, E.; Petitclerc, E.; Gaudreault, R. C. Quick and simple detection technique to assess the binding of antimicrotubule agents to the colchicine-binding site. *Biol. Proced. Online* **2010**, *12*, 113−117.
(37) Medrano, F. J.; Andreu, J. M.; Gorbunoff, M. J.; Timasheff, S. N. Roles of colchicine ring-B and ring-C in the binding process to tubulin. *Biochemistry (Moscow)* **1989**, *28*, 5589−5599.
(38) Medrano, F. J.; Andreu, J. M.; Gorbunoff, M. J.; Timasheff, S. N. Roles of ring-C oxygens in the binding of colchicine to tubulin. *Biochemistry (Moscow)* **1991**, *30*, 3770−3777.
(39) Barbier, P.; Peyrot, V.; Leynadier, D.; Andreu, J. M. The active GTP- and ground GDP-liganded states of tubulin are distinguished by the binding of chiral isomers of ethyl 5-amino-2-methyl-1,2-dihydro-3-phenylpyrido 3,4-b pyrazin-7-yl carbamate. *Biochemistry (Moscow)* **1998**, *37*, 758−768.
(40) Barbier, P.; Dorleans, A.; Devred, F.; Sanz, L.; Allegro, D.; Alfonso, C.; Knossow, M.; Peyrot, V.; Andreu, J. M. Stathmin and interfacial microtubule inhibitors recognize a naturally curved conformation of tubulin dimers. *J. Biol. Chem.* **2010**, *285*, 31672−31681.
(41) Medrano, F. J.; Andreu, J. M.; Gorbunoff, M. J.; Timasheff, S. N. Roles of ring C oxygens in the binding of colchicine to tubulin. *Biochemistry* **1991**, *30*, 3770−7.
(42) Díaz, J. F.; Buey, R. M. Characterizing ligand-microtubule binding by competition methods. In *Methods in Molecular Medicine*; Zhou, J., Ed.; Humana Press Inc.: Totowa, NJ, 2007; Vol. *137*, pp 245−260.
(43) Leynadier, D.; Peyrot, V.; Sarrazin, M.; Briand, C.; Andreu, J. M.; Rener, G. A.; Temple, C., Jr. Tubulin binding of two 1-deaza-7,8-dihydropteridines with different biological properties: Enantiomers NSC 613862 (*S*)-(−) and NSC 613863 (*R*)-(+). *Biochemistry* **1993**, *32*, 10675−82.
(44) Xu, K.; Schwarz, P. M.; Luduena, R. F. Interaction of nocodazole with tubulin isotypes. *Drug Dev. Res.* **2002**, *55*, 91−96.
(45) Cortese, F.; Bhattacharyya, B.; Wolff, J. Podophyllotoxin as a probe for colchicine binding-site of tubulin. *J. Biol. Chem.* **1977**, *252*, 1134−1140.
(46) Diaz, J. F.; Andreu, J. M. Kinetics of dissociation of the tubulin−colchicine complex—Complete reaction scheme and comparison to thermodynamic measurements. *J. Biol. Chem.* **1991**, *266*, 2890−2896.
(47) Mooberry, S. L.; Weiderhold, K. N.; Dakshanamurthy, S.; Hamel, E.; Banner, E. J.; Kharlamova, A.; Hempel, J.; Gupton, J. T.; Brown, M. L. Identification and characterization of a new tubulin-binding tetrasubstituted brominated pyrrole. *Mol. Pharmacol.* **2007**, *72*, 132−140.
(48) (a) Ganguly, A.; Yang, H.; Saharma, R.; Patel, K. D.; Cabral, F. The role of microtubules and their dynamics in cell migration. *J. Biol. Chem.* **2012**, *21*, 43359−43369. (b) Zheng, S.; Zhong, Q.; Jiang, Q.; Mottamal, M.; Zhang, Q.; Zhu, N.; Burrow, M. E.; Worthylake, R. A.; Wang, G. Discovery of a series of thiazole derivatives as novel inhibitors of metastatic cancer cell migration and invasion. *ACS Med. Chem. Lett.* **2013**, *4*, 191−196.
(49) Andreu, J. M. Tubulin purification. In *Methods in Molecular Medicine*; Zhou, J., Ed.; Humana Press Inc.: Totowa, NJ, 2007; Vol. *137*, pp 17−28.
(50) Fitzgerald, T. J. Molecular features of colchicine associated with antimitotic activity and inhibition of tubulin polymerization. *Biochem. Pharmacol.* **1976**, *25*, 1383−7.
(51) Temple, C.; Rener, G. A.; Comber, R. N. New anticancer agents—Alterations of the carbamate group of ethyl (5-amino-1,2-dihydro-3-phenylpyrido-3,4-*b*-pyrazin-7-yl)carbamates. *J. Med. Chem.* **1989**, *32*, 2363−2367.